Figure 3

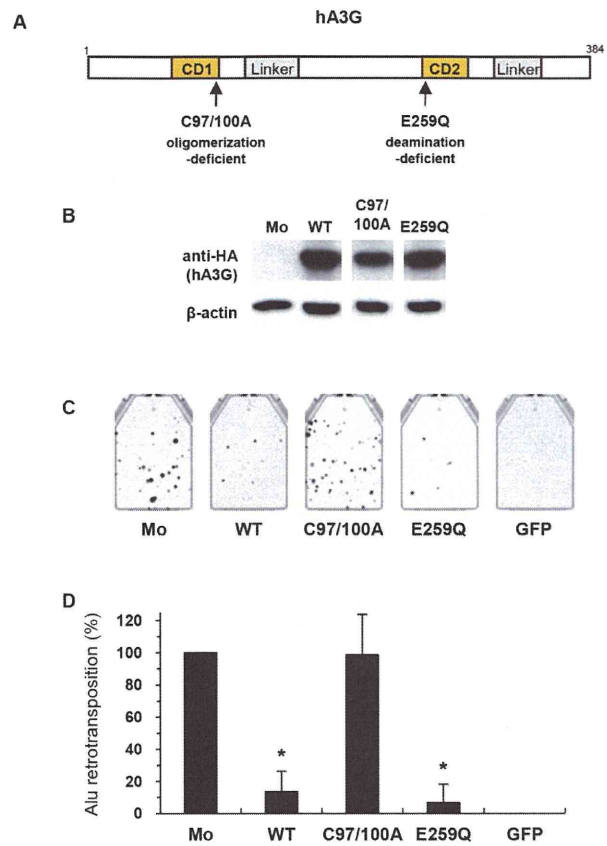

Figure 3. The anti-Alu activity of hA3G is associated with its oligomerization and is independent of its deaminase activity. (**A**) Schematic depiction of two mutants: an oligomerization-deficient mutant, C97/100A, and a deamination-deficient mutant, E259Q. (**B**) Western blot analysis was performed using extracts from 293T cells transfected with plasmids expressing HA-tagged hA3G mutant proteins. Monoclonal antibodies specific for HA (upper) or β-actin (lower) were used. (**C**, **D**) An *Alu* retrotransposition assay was performed as described in Figure 1. A GFP expression vector was used as a negative control. Crystal violet-stained $G418^R$ colonies were counted to determine the level of *Alu* retrotransposition. The data shown are the mean ± SD of triplicate experiments. Mo, mock; WT, wild-type hA3G; GFP, GFP only. $^*P < 0.005$, *t*-test.

doi: 10.1371/journal.pone.0084228.g003

(Y124, Y125, F126, and W127) that have been predicted to be hot spots of protein–protein interaction [68] and have been reported to be critical for the RNA-mediated oligomerization of hA3G [34,59]. The structural model of hA3G-4G(124–127) indicates that the mutant does not form the aromatic cluster, leaving a prominent space between two monomers (compare

Oligomerized hA3G inhibits retrotransposition

Figure 4

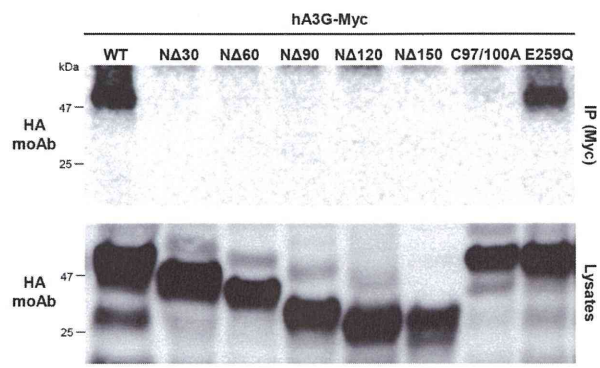

Figure 4. The homooligomerization of hA3G is dependent on the N-terminal 30 amino acid residues of this protein. 293T cells cotransfected with the Myc-tagged and HA-tagged hA3G expression plasmids were immunoprecipitated (IP) with an anti-Myc polyclonal antibody. The resulting complexes were analyzed by immunoblotting with a monoclonal antibody against the HA tag to detect oligomerized hA3G (upper). Cell lysate aliquots were also analyzed in parallel by immunoblotting for the HA tag (lower). WT, wild-type hA3G.

doi: 10.1371/journal.pone.0084228.g004

the left and right panels of Figure 6C and the left and right panels of Figure 6D). Given this result, we then introduced in silico mutations into the five-amino-acid cluster (R24, P25, I26, L27, and S28) of the putative dimer interface (RPILS –> GGGGG; designated 5G(24–28)) (compare the left and right panels of Figure 6E and the left and right panels of Figure 6F). The space between the two monomers of the mutant was clearly comparable to that of 4G(124–127), implying that the 5G(24–28) mutant cannot form a dimer. Based on the structural models, we constructed the myc-tagged N-terminal mutants hA3G-5G(24–28) and hA3G-4G(124–127) to determine whether the former hA3G mutant is unable to physically oligomerize. To assess oligomerization, we performed coimmunoprecipitation-based oligomerization assays using wild-type and mutant hA3G proteins. The 5G(24–28) mutant was not coimmunoprecipitated (Figure 6G), nor was 4G(124–127), suggesting that these mutants do not have the ability to oligomerize. Finally, to determine whether the 4G(124–127) and 5G(24–28) mutants lacks anti-*Alu* activity, we performed the retrotransposition assay and found out that these mutants had completely lost the ability to inhibit *Alu* retrotransposition (Figure 6H). hA3G mutants harboring individual amino acid substitutions (R24G and Y125G) displayed equivalent or moderately less inhibitory activity with comparable dimerization (Figures S3A and S3B). In addition, 5G(24–28) and 4G(124–127) mutations both negatively affect the ability of hA3G to inhibit HIV-1 infection (Figure S4). Taken altogether, these results indicate that the N-terminal amino acid residues 24–28 (RPILS) contribute to the oligomerization of hA3G and its anti-*Alu* retrotransposition activity.

Figure 5

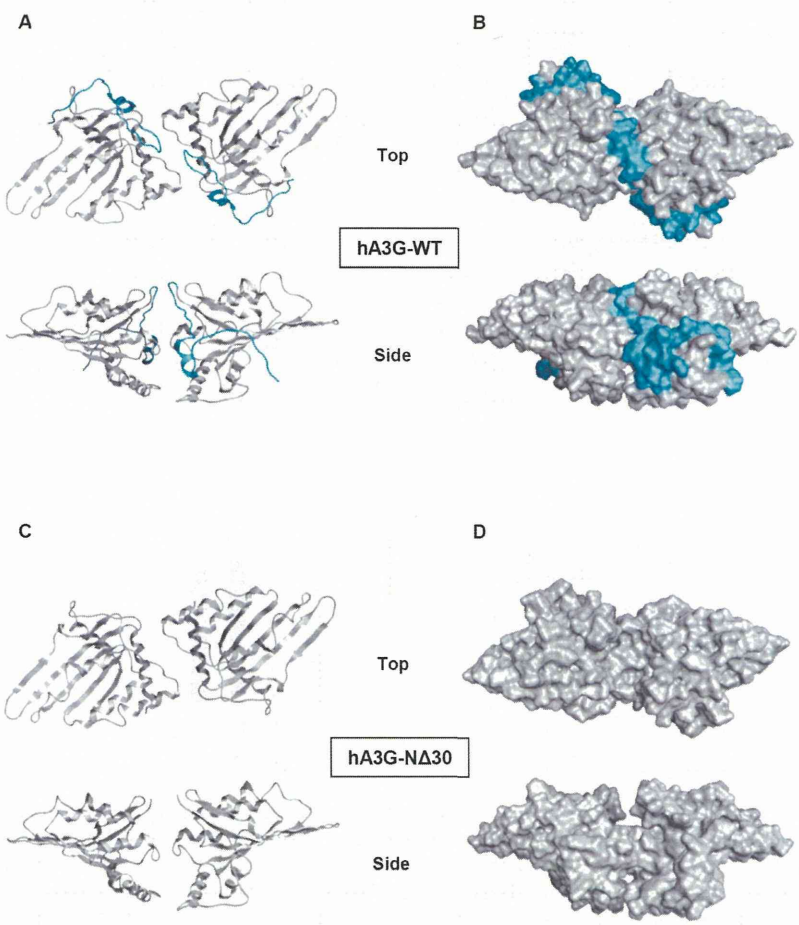

Figure 5. The N-terminal 30 amino acids of hA3G are located at the dimer interface and are therefore key residues for the oligomerization of hA3G. Structural models of the hA3G N-terminal domain. The models were constructed by homology modeling using the X-ray crystal structure of hA2. The head-to-head dimer structure of hA3G N-terminal domain is represented by ribbon models (A and C) and space-filling models (B and D). (**A**, **B**) Views of the top (upper) and side (lower) of wild-type (WT) hA3G. Cyan, N-terminal 30 amino acids of hA3G. (**C**, **D**) Views of the top (upper) and side (lower) of the N-terminal 30-amino-acid deletion mutant of hA3G.

doi: 10.1371/journal.pone.0084228.g005

Figure 6

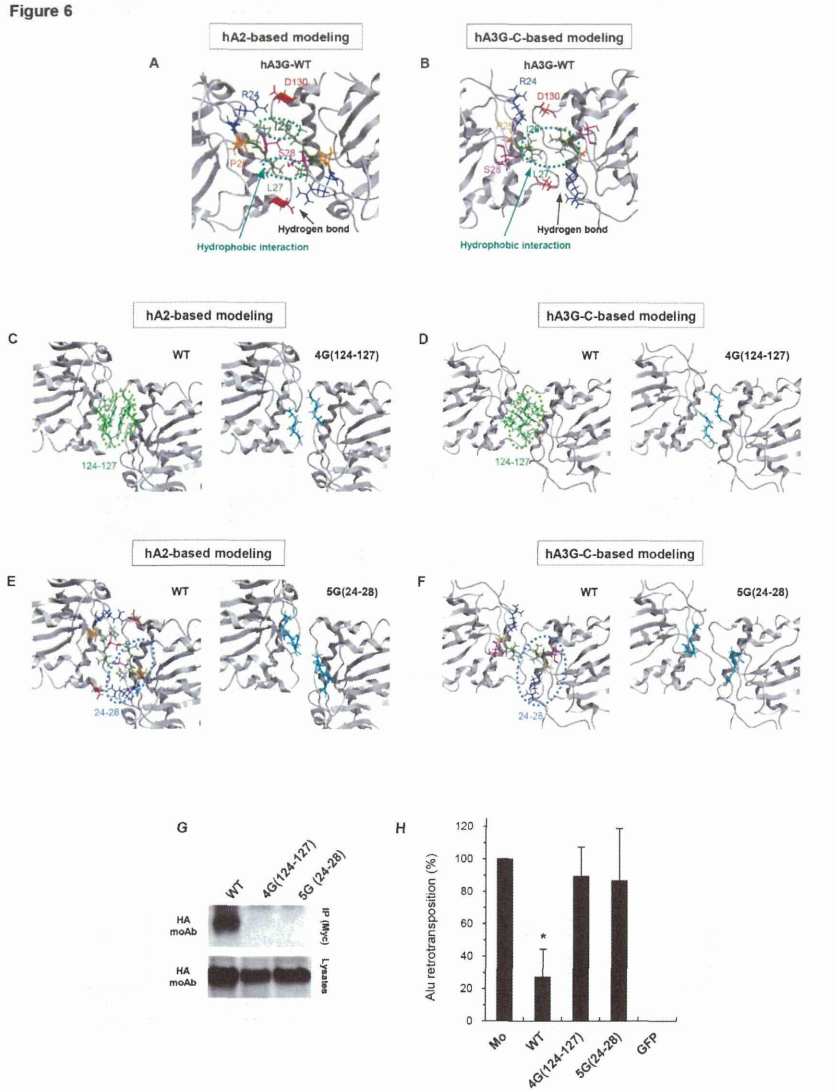

Figure 6. Residues 24–28, as well as known residues 124–127, contribute to the ability of hA3G to homooligomerize and its inhibitory activity against Alu retrotransposition. (A–F) Structural models of hA3G dimer based on the human APOBEC2 (hA2) crystal structure (A, C, and E) and the C-terminal hA3G (hA3G-C) NMR structure (B, D, and F). (**A**, **B**) The interaction surface of the hA3G N-terminal domain in the head-to-head dimer is shown. The hydrophobic interactions formed between either I26 or L27 (green) and their counterpart residues of another monomer (green) are encircled by green dotted lines. A hydrogen bond is formed between a basic residue R24 (blue) and another monomer's D130 (red). Another hydrogen bond is formed between the S28 residues (pink) of two monomers. Structural stability may be conferred by P25 (orange). (**C**, **D**) The dimer interface at amino acid residues 124–127. Left panel, the aromatic amino acid cluster (YYFW) at positions 124–127 is depicted in light green; right panel, the substitution of these residues with glycines is shown in cyan. (**E**, **F**) The dimer interface at amino acid residues 24–28. Left panel, the dimer interface residues (RPILS) at positions 24–28 are depicted in colors similar to those in A; right panel, substitution of these residues with glycines is shown in cyan. (**G**) IP-Western blot analysis was performed as described in Figure 4; upper, IP; lower, cell lysates. (**H**) An *Alu* retrotransposition assay was performed as described in Figure 1. Crystal violet-stained G418R colonies were counted to determine the level of *Alu* retrotransposition. The data shown are the mean ±SD of triplicate experiments. Mo, mock; WT, wild-type hA3G; GFP, GFP only. *P < 0.05, **P < 0.005, t-test.

doi: 10.1371/journal.pone.0084228.g006

hA3G oligomerization is associated with the inhibition of L1 retrotransposition

The inhibitory effects of the hA3G protein on *Alu* retrotransposition resembles its effects on L1 retrotransposition in two regards, first, that hA3G showed similar levels of inhibitory activity against the both retrotransposition events (Figure 1C and ref [37,40]), and second, that the hA3G restriction of retrotransposition is independent of deamination in both cases (Figure 3C and refs. 35,37). These similarities prompted us to determine whether the inhibition of L1 retrotransposition by hA3G requires hA3G oligomerization, as does the inhibition of *Alu* retrotransposition. We performed an L1 retrotransposition assay using all hA3G mutants that we created in this study. As expected, the mutants that do not form oligomers, including NΔ30, NΔ60, NΔ90, NΔ120, NΔ150, C97/100A, 5G(24–28), and 4G(124–127), did not inhibit L1 retrotransposition (Figure 7A, 7B, and 7C), whereas, as observed for *Alu* retrotransposition in Figure 3C, the E259Q deamination mutant had a wild-type level of anti-L1 activity (Figure 7B). Thus, the inhibitory effect of hA3G on *Alu* retrotransposition is associated with hA3G oligomerization but independent of its deaminase activity. We therefore postulate that the inhibitory activities of hA3G against *Alu* and L1 retrotransposition might share common mechanism(s).

Discussion

Our present study demonstrated that hA3 family proteins inhibit *Alu* retrotransposition at differential levels, which are very similar to the levels at which these host proteins block L1 retrotransposition. With respect to hA3G, the N-terminal 30 amino acids are important for the anti-*Alu* activity. The ability of hA3G to inhibit *Alu* retrotransposition was independent of its deaminase activity but associated with its oligomerization activity, as previously reported by Hulme et al. [35] and Bulliard et al. [34], respectively. In agreement with these findings, we found that the N-terminal 30 amino acids that are responsible for counteracting *Alu* retrotransposition are required for the oligomerization of this protein. We used structural modeling to identify the specific residues among the N-terminal 30 amino acids that are responsible for the oligomerization of hA3G. We finally identified amino acid residues 24–28 of hA3G as the contributors of oligomerization.

Importantly, these residues were also critical for the inhibitory activity of L1 retrotransposon, suggesting that this activity might involve the same mechanism as that of *Alu* retrotransposition. This hypothesis makes sense because *Alu* elements do not encode a functional reverse transcriptase or endonuclease, and therefore, they need to hijack the L1-encoded enzymatic machinery for retrotransposition through mechanisms that are currently unclear. It is intriguing to speculate that hA3G might be able to physically block both the *Alu* and L1 retroelements because hA3G is intrinsically an RNA-binding protein that can associate non-specifically with cellular RNAs [48,59,65,69], including those derived from *Alu* retroelements [34,70], or because this protein might directly interact with the L1 ORF2 protein. It is likely that both cases would result in the effective inhibition of *Alu* reverse transcription, and are dependent on the ability of hA3G to form oligomers. In the former case, *Alu* RNA *per se* might help stabilize hA3G oligomer formation, as suggested in Figure S2.

It was somewhat unexpected to find that the N-terminal 30 amino acids of hA3G are required for oligomerization in our study because amino acid positions 124/127 have previously been reported to be important [34,58,59]. Indeed, although only minor effects of either a single R24 or S28 mutation on oligomerization were shown by Huthoff et al. [59] and Bulliard et al. [34] (the former of which was confirmed in Figure S3A), respectively, our study revealed that the previously unappreciated amino acid positions 24–28 among these first 30 residues are responsible for the ability of hA3G to homooligomerize. The dependence of oligomerization on these residues is most likely because not only the amino acids R24 and S28 but also the residues between them are involved in the formation of the interaction interface of an hA3G dimer, as shown in our structural models (Figure 6). This study also reveals that both the amino acid residues 24–28 and 124–127 are equally important for the oligomerization of hA3G. Regarding this point, we assume that the lack or a functional defect of a single interaction interface would be able to totally abolish the protein-protein interaction by leading to the structural destabilization.

Whereas transcriptional repressors such as SRY, SOX2 and methyl-CpG-binding protein 2 have been reported to negatively regulate L1 retrotransposition at the transcriptional levels [71-73], post-transcriptional L1 regulation (apart from that by endogenously encoded small interfering RNAs [74]) like premature polyadenylation and aberrant splicing of its mRNA was also shown to result in a negative influence on L1 expression [75]. In the latter case, retrotransposition-incompetent L1 elements that encode intact ORF2 protein are still able to create DNA double-strand breaks [76] and therefore keep mobilizing *Alu* elements [5,53]. Particularly in such conditions, hA3 proteins would play pivotal roles in the inhibition of *Alu* retrotransposition, putatively through binding to either the ORF2 protein or *Alu* RNA as described above.

It should be noted that the superfamily-1 RNA helicase protein MOV10 (Moloney Leukemia Virus 10; for review, see ref[77].), which is highly conserved across a wide range of species, has recently been reported to inhibit not only infection by several retroviruses, such as HIV-1, simian immunodeficiency virus, murine leukemia virus, and equine infectious anemia virus [78,79], but also the retrotransposition of endogenous retroelements [80-82], exactly as hA3G does. Most importantly, MOV10 was identified to be a protein interacting with hA3G in an RNA-dependent manner [83], suggesting that these two proteins may play mutually supporting roles in restricting exogenous viruses and endogenous retroelements. Further analyses are required to elucidate the precise mechanisms by which hA3 family proteins negatively regulate *Alu* and L1 retrotransposition, possibly in cooperation with other cellular factor(s).

Figure 7

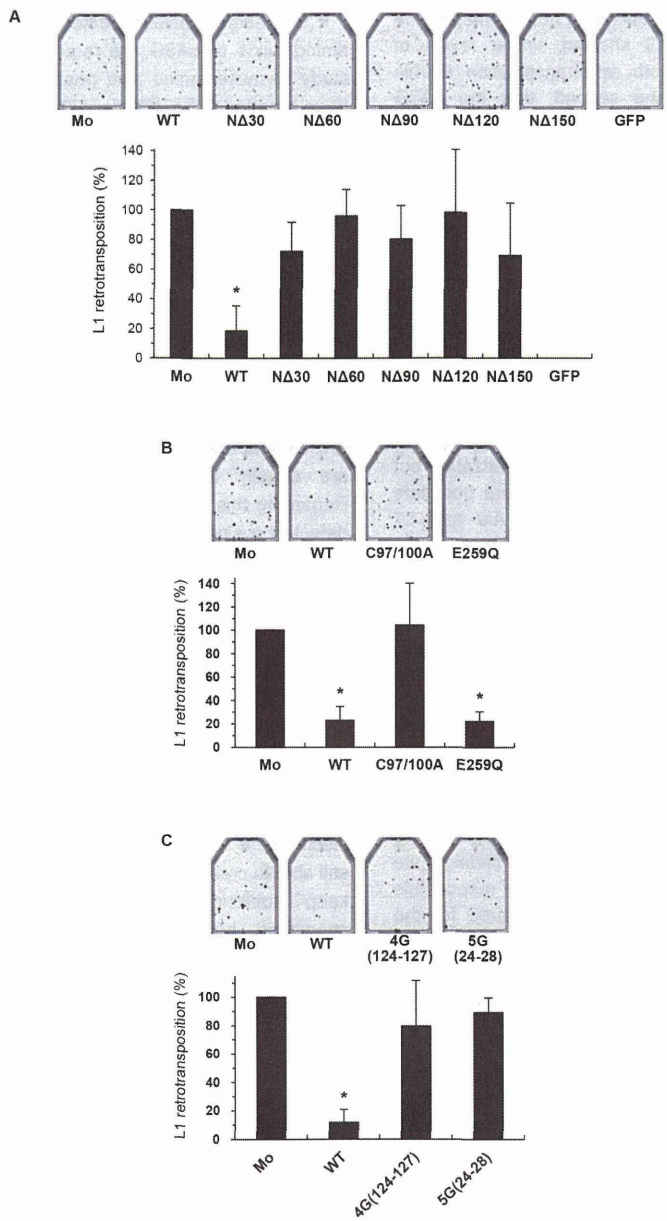

Figure 7. The oligomerization of hA3G is also associated with its anti-L1 activity. HeLa cells were cotransfected with the *neo*^{r}-based L1 expression vector pCEP4/L1mneoI/ColE1 and either a wild-type (WT) or mutant hA3G expression plasmids. Seventy-two hours later, cells were trypsinized, re-seeded into T25 or T75 flasks, and subjected to G418 (1 mg/ml) selection. At 14 days after selection, the resultant G418^R colonies fixed, stained with crystal violet, and counted to determine the level of L1 retrotransposition. (**A**) Compare the results with Figure 2D and 2E. (**B**) Compare the results with Figure 3C and 3D. (**C**) Compare the results with Figure 6H. The data shown are the mean ± SD of triplicate experiments. Mo, mock; WT, wild-type hA3G; GFP, GFP only. *$P < 0.005$, *t*-test.

doi: 10.1371/journal.pone.0084228.g007

Supporting Information

Figure S1. Inhibitory effect of hA3G deletion mutants on HIV-1 infection was evaluated by cotransfecting 293T cells with hA3G and VSV-G plasmids, together with a luciferase-based Vif (-) Env (-) HIV-1 construct, as described by Iwabu et al. (J. Biol. Chem., 285: 35350-8, 2010).
After 48 h, each viral supernatant was harvested. Normalized supernatants were incubated with 293T cells for additional 48 h. Cells were then lysed and subjected to luciferase assay. The data shown are the mean ± SD of triplicate experiments. RLU: relative light units.
(TIF)

Figure S2. Cellular RNA contributes to the stabilization of hA3G's oligomer. HA-tagged hA3G-WT in the immunoprecipitate as described in Figure 4, with or without RNase A treatment.
(TIF)

Figure S3. hA3G mutants with individual amino acid substitutions. (A) Oligomerization assay was performed by IP-Western blot analysis, as described in Figure 4; upper, IP; lower, cell lysates. (B) An *Alu* retrotransposition assay was performed as described in Figure 1. Crystal violet-stained $G418^R$ colonies were counted to determine the level of *Alu* retrotransposition. The data shown are the mean ±SD of triplicate experiments. Mo, mock; WT, wild-type hA3G; GFP, GFP only. $^*P < 0.05$, $^{**}P < 0.005$, *t*-test.
(TIF)

Figure S4. Inhibitory effect of hA3G oligomerization mutant proteins on HIV-1 infection. The assay was performed as described in Figure S1. The data shown are the mean ± SD of triplicate experiments. RLU: relative light units.
(TIF)

Acknowledgements

We thank Astrid M. Roy-Engel, Nicolas Gilbert, and Thierry Heidmann for the generous gifts of expression plasmids.

Author Contributions

Conceived and designed the experiments: KT. Performed the experiments: TK JFA YI MY HF. Analyzed the data: TK JFA YI MY HS HF KT. Wrote the manuscript: KT.

References

1. Lander ES, Linton LM, Birren B, Nusbaum C, Zody MC et al. (2001) Initial sequencing and analysis of the human genome. Nature 409: 860-921. doi:10.1038/35057062. PubMed: 11237011.
2. Hohjoh H, Singer MF (1996) Cytoplasmic ribonucleoprotein complexes containing human LINE-1 protein and RNA. EMBO J 15: 630-639. PubMed: 8599946.
3. Martin SL (1991) Ribonucleoprotein particles with LINE-1 RNA in mouse embryonal carcinoma cells. Mol Cell Biol 11: 4804-4807. PubMed: 1715025.
4. Cost GJ, Feng Q, Jacquier A, Boeke JD (2002) Human L1 element target-primed reverse transcription in vitro. EMBO J 21: 5899-5910. doi: 10.1093/emboj/cdf592. PubMed: 12411507.
5. Dewannieux M, Esnault C, Heidmann T (2003) LINE-mediated retrotransposition of marked Alu sequences. Nat Genet 35: 41-48. doi: 10.1038/ng1223. PubMed: 12897783.
6. Claverie-Martín F, Flores C, Antón-Gamero M, González-Acosta H, García-Nieto V (2005) The Alu insertion in the CLCN5 gene of a patient with Dent's disease leads to exon 11 skipping. J Hum Genet 50: 370-374. doi:10.1007/s10038-005-0265-5. PubMed: 16041495.
7. Li X, Scaringe WA, Hill KA, Roberts S, Mengos A et al. (2001) Frequency of recent retrotransposition events in the human factor IX gene. Hum Mutat 17: 511-519. doi:10.1002/humu.1134. PubMed: 11385709.
8. Meischl C, Boer M, Ahlin A, Roos D (2000) A new exon created by intronic insertion of a rearranged LINE-1 element as the cause of chronic granulomatous disease. Eur J Hum Genet 8: 697-703. doi: 10.1038/sj.ejhg.5200523. PubMed: 10980575.
9. Oldridge M, Zackai EH, McDonald-McGinn DM, Iseki S, Morriss-Kay GM et al. (1999) De novo alu-element insertions in FGFR2 identify a distinct pathological basis for Apert syndrome. Am J Hum Genet 64: 446-461. doi:10.1086/302245. PubMed: 9973282.
10. Yoshida K, Nakamura A, Yazaki M, Ikeda S, Takeda S (1998) Insertional mutation by transposable element, L1, in the DMD gene results in X-linked dilated cardiomyopathy. Hum Mol Genet 7: 1129-1132. doi:10.1093/hmg/7.7.1129. PubMed: 9618170.
11. Narita N, Nishio H, Kitoh Y, Ishikawa Y, Ishikawa Y et al. (1993) Insertion of a 5' truncated L1 element into the 3' end of exon 44 of the dystrophin gene resulted in skipping of the exon during splicing in a case of Duchenne muscular dystrophy. J Clin Invest 91: 1862-1867. doi:10.1172/JCI116402. PubMed: 8387534.
12. Wallace MR, Andersen LB, Saulino AM, Gregory PE, Glover TW et al. (1991) A de novo Alu insertion results in neurofibromatosis type 1. Nature 353: 864-866. doi:10.1038/353864a0. PubMed: 1719426.
13. Kazazian HH Jr., Wong C, Youssoufian H, Scott AF, Phillips DG et al. (1988) Haemophilia A resulting from de novo insertion of L1 sequences represents a novel mechanism for mutation in man. Nature 332: 164-166. doi:10.1038/332164a0. PubMed: 2831458.
14. Baillie JK, Barnett MW, Upton KR, Gerhardt DJ, Richmond TA et al. (2011) Somatic retrotransposition alters the genetic landscape of the human brain. Nature 479: 534-537. doi:10.1038/nature10531. PubMed: 22037309.
15. Coufal NG, Garcia-Perez JL, Peng GE, Yeo GW, Mu Y et al. (2009) L1 retrotransposition in human neural progenitor cells. Nature 460: 1127-1131. doi:10.1038/nature08248. PubMed: 19657334.
16. Economou-Pachnis A, Lohse MA, Furano AV, Tsichlis PN (1985) Insertion of long interspersed repeated elements at the Igh (immunoglobulin heavy chain) and Mlvi-2 (Moloney leukemia virus integration 2) loci of rats. Proc Natl Acad Sci U S A 82: 2857-2861. doi: 10.1073/pnas.82.9.2857. PubMed: 2986141.
17. Morse B, Rotherg PG, South VJ, Spandorfer JM, Astrin SM (1988) Insertional mutagenesis of the myc locus by a LINE-1 sequence in a human breast carcinoma. Nature 333: 87-90. doi:10.1038/333087a0. PubMed: 2834650.
18. Miki Y, Nishisho I, Horii A, Miyoshi Y, Utsunomiya J et al. (1992) Disruption of the APC gene by a retrotransposal insertion of L1 sequence in a colon cancer. Cancer Res 52: 643-645. PubMed: 1310068.
19. Shukla R, Upton Kyle R, Muñoz-Lopez M, Gerhardt Daniel J, Fisher Malcolm E et al. (2013) Endogenous Retrotransposition Activates Oncogenic Pathways in Hepatocellular Carcinoma. Cell 153: 101-111. doi:10.1016/j.cell.2013.02.032. PubMed: 23540693.
20. Sheehy AM, Gaddis NC, Choi JD, Malim MH (2002) Isolation of a human gene that inhibits HIV-1 infection and is suppressed by the viral Vif protein. Nature 418: 646-650. doi:10.1038/nature00939. PubMed: 12167863.
21. Harris RS, Bishop KN, Sheehy AM, Craig HM, Petersen-Mahrt SK et al. (2003) DNA deamination mediates innate immunity to retroviral infection. Cell 113: 803-809. doi:10.1016/S0092-8674(03)00423-9. PubMed: 12809610.
22. Mangeat B, Turelli P, Caron G, Friedli M, Perrin L et al. (2003) Broad antiretroviral defence by human APOBEC3G through lethal editing of

nascent reverse transcripts. Nature 424: 99-103. doi:10.1038/nature01709. PubMed: 12808466.
23. Zhang H, Yang B, Pomerantz RJ, Zhang C, Arunachalam SC et al. (2003) The cytidine deaminase CEM15 induces hypermutation in newly synthesized HIV-1 DNA. Nature 424: 94-98. doi:10.1038/nature01707. PubMed: 12808465.
24. Mariani R, Chen D, Schröfelbauer B, Navarro F, König R et al. (2003) Species-specific exclusion of APOBEC3G from HIV-1 virions by Vif. Cell 114: 21-31. doi:10.1016/S0092-8674(03)00515-4. PubMed: 12859895.
25. Bogerd HP, Doehle BP, Wiegand HL, Cullen BR (2004) A single amino acid difference in the host APOBEC3G protein controls the primate species specificity of HIV type 1 virion infectivity factor. Proc Natl Acad Sci U S A 101: 3770-3774. doi:10.1073/pnas.0307713101. PubMed: 14999100.
26. Mangeat B, Turelli P, Liao S, Trono D (2004) A single amino acid determinant governs the species-specific sensitivity of APOBEC3G to Vif action. J Biol Chem 279: 14481-14483. doi:10.1074/jbc.C400060200. PubMed: 14966139.
27. Schröfelbauer B, Chen D, Landau NR (2004) A single amino acid of APOBEC3G controls its species-specific interaction with virion infectivity factor (Vif). Proc Natl Acad Sci U S A 101: 3927-3932. doi:10.1073/pnas.0307132101. PubMed: 14978281.
28. Russell RA, Wiegand HL, Moore MD, Schäfer A, McClure MO et al. (2005) Foamy virus Bet proteins function as novel inhibitors of the APOBEC3 family of innate antiretroviral defense factors. J Virol 79: 8724-8731. doi:10.1128/JVI.79.14.8724-8731.2005. PubMed: 15994766.
29. Delebecque F, Suspène R, Calattini S, Casartelli N, Saïb A et al. (2006) Restriction of foamy viruses by APOBEC cytidine deaminases. J Virol 80: 605-614. doi:10.1128/JVI.80.2.605-614.2006. PubMed: 16378963.
30. Sasada A, Takaori-Kondo A, Shirakawa K, Kobayashi M, Abudu A et al. (2005) APOBEC3G targets human T-cell leukemia virus type 1. Retrovirology 2: 32. doi:10.1186/1742-4690-2-S1-S32. PubMed: 15943885.
31. Kobayashi M, Takaori-Kondo A, Shindo K, Abudu A, Fukunaga K et al. (2004) APOBEC3G targets specific virus species. J Virol 78: 8238-8244. doi:10.1128/JVI.78.15.8238-8244.2004. PubMed: 15254195.
32. Okeoma CM, Lovsin N, Peterlin BM, Ross SR (2007) APOBEC3 inhibits mouse mammary tumour virus replication in vivo. Nature 445: 927-930. doi:10.1038/nature05540. PubMed: 17259974.
33. Esnault C, Heidmann O, Delebecque F, Dewannieux M, Ribet D et al. (2005) APOBEC3G cytidine deaminase inhibits retrotransposition of endogenous retroviruses. Nature 433: 430-433. doi:10.1038/nature03238. PubMed: 15674295.
34. Bulliard Y, Turelli P, Röhrig UF, Zoete V, Mangeat B et al. (2009) Functional analysis and structural modeling of human APOBEC3G reveal the role of evolutionarily conserved elements in the inhibition of human immunodeficiency virus type 1 infection and Alu transposition. J Virol 83: 12611-12621. doi:10.1128/JVI.01491-09. PubMed: 19776130.
35. Hulme AE, Bogerd HP, Cullen BR, Moran JV (2007) Selective inhibition of Alu retrotransposition by APOBEC3G. Gene 390: 199-205. doi:10.1016/j.gene.2006.08.032. PubMed: 17079095.
36. Chiu YL, Witkowska HE, Hall SC, Santiago M, Soros VB et al. (2006) High-molecular-mass APOBEC3G complexes restrict Alu retrotransposition. Proc Natl Acad Sci U S A 103: 15588-15593. doi:10.1073/pnas.0604524103. PubMed: 17030807.
37. Kinomoto M, Kanno T, Shimura M, Ishizaka Y, Kojima A et al. (2007) All APOBEC3 family proteins differentially inhibit LINE-1 retrotransposition. Nucleic Acids Res 35: 2955-2964. doi:10.1093/nar/gkm181. PubMed: 17439959.
38. Ikeda T, Abd El Galil KH, Tokunaga K, Maeda K, Sata T et al. (2011) Intrinsic restriction activity by apolipoprotein B mRNA editing enzyme APOBEC1 against the mobility of autonomous retrotransposons. Nucleic Acids Res 39: 5538-5554. doi:10.1093/nar/gkr124. PubMed: 21398638.
39. Khatua AK, Taylor HE, Hildreth JE, Popik W (2010) Inhibition of LINE-1 and Alu retrotransposition by exosomes encapsidating APOBEC3G and APOBEC3F. Virology 400: 68-75. doi:10.1016/j.virol.2010.01.021. PubMed: 20153011.
40. Niewiadomska AM, Tian C, Tan L, Wang T, Sarkis PTN et al. (2007) Differential Inhibition of Long Interspersed Element 1 by APOBEC3 Does Not Correlate with High-Molecular-Mass-Complex Formation or P-Body Association. J Virol 81: 9577-9583. doi:10.1128/JVI.02800-06. PubMed: 17582006.
41. Arias JF, Koyama T, Kinomoto M, Tokunaga K (2012) Retroelements versus APOBEC3 family members: No great escape from the magnificent seven. Front Microbiol 3: 275. PubMed: 22912627.
42. Turelli P, Mangeat B, Jost S, Vianin S, Trono D (2004) Inhibition of hepatitis B virus replication by APOBEC3G. Science 303: 1829. doi:10.1126/science.1092066. PubMed: 15031497.
43. Noguchi C, Ishino H, Tsuge M, Fujimoto Y, Imamura M et al. (2005) G to A hypermutation of hepatitis B virus. Hepatology 41: 626-633. doi:10.1002/hep.20580. PubMed: 15726649.
44. OhAinle M, Kerns JA, Malik HS, Emerman M (2006) Adaptive evolution and antiviral activity of the conserved mammalian cytidine deaminase APOBEC3H. J Virol 80: 3853-3862. doi:10.1128/JVI.80.8.3853-3862.2006. PubMed: 16571802.
45. Sawyer SL, Emerman M, Malik HS (2004) Ancient adaptive evolution of the primate antiviral DNA-editing enzyme APOBEC3G. PLoS Biol 2: E275. doi:10.1371/journal.pbio.0020275. PubMed: 15269786.
46. Schumann GG (2007) APOBEC3 proteins: major players in intracellular defence against LINE-1-mediated retrotransposition. Biochem Soc Trans 35: 637-642. doi:10.1042/BST0350637. PubMed: 17511669.
47. Stenglein MD, Harris RS (2006) APOBEC3B and APOBEC3F inhibit L1 retrotransposition by a DNA deamination-independent mechanism. J Biol Chem 281: 16837-16841. doi:10.1074/jbc.M602367200. PubMed: 16648136.
48. Muckenfuss H, Hamdorf M, Held U, Perkovic M, Löwer J et al. (2006) APOBEC3 proteins inhibit human LINE-1 retrotransposition. J Biol Chem 281: 22161-22172. doi:10.1074/jbc.M601716200. PubMed: 16735504.
49. Bogerd HP, Wiegand HL, Hulme AE, Garcia-Perez JL, O'Shea KS et al. (2006) Cellular inhibitors of long interspersed element 1 and Alu retrotransposition. Proc Natl Acad Sci U S A 103: 8780-8785. doi:10.1073/pnas.0603313103. PubMed: 16728505.
50. Turelli P, Vianin S, Trono D (2004) The innate antiretroviral factor APOBEC3G does not affect human LINE-1 retrotransposition in a cell culture assay. J Biol Chem 279: 43371-43373. doi:10.1074/jbc.C400334200. PubMed: 15322092.
51. Tan L, Sarkis PT, Wang T, Tian C, Yu XF (2009) Sole copy of Z2-type human cytidine deaminase APOBEC3H has inhibitory activity against retrotransposons and HIV-1. FASEB J 23: 279-287. doi:10.1096/fj.07-088781. PubMed: 18827027.
52. Gilbert N, Lutz-Prigge S, Moran JV (2002) Genomic deletions created upon LINE-1 retrotransposition. Cell 110: 315-325. doi:10.1016/S0092-8674(02)00828-0. PubMed: 12176319.
53. Wallace N, Wagstaff BJ, Deininger PL, Roy-Engel AM (2008) LINE-1 ORF1 protein enhances Alu SINE retrotransposition. Gene 419: 1-6. doi:10.1016/j.gene.2008.04.007. PubMed: 18534786.
54. Iwabu Y, Fujita H, Kinomoto M, Kaneko K, Ishizaka Y et al. (2009) HIV-1 accessory protein Vpu internalizes cell-surface BST-2/tetherin through transmembrane interactions leading to lysosomes. J Biol Chem 284: 35060-35072. doi:10.1074/jbc.M109.058305. PubMed: 19837671.
55. Iwabu Y, Kinomoto M, Tatsumi M, Fujita H, Shimura M et al. (2010) Differential anti-APOBEC3G activity of HIV-1 Vif proteins derived from different subtypes. J Biol Chem 285: 35350-35358. doi:10.1074/jbc.M110.173286. PubMed: 20833716.
56. Prochnow C, Bransteitter R, Klein MG, Goodman MF, Chen XS (2007) The APOBEC-2 crystal structure and functional implications for the deaminase AID. Nature 445: 447-451. doi:10.1038/nature05492. PubMed: 17187054.
57. Chen KM, Harjes E, Gross PJ, Fahmy A, Lu Y et al. (2008) Structure of the DNA deaminase domain of the HIV-1 restriction factor APOBEC3G. Nature 452: 116-119. doi:10.1038/nature06638. PubMed: 18288108.
58. Lavens D, Peelman F, Van der Heyden J, Uyttendaele I, Catteeuw D et al. (2010) Definition of the interacting interfaces of Apobec3G and HIV-1 Vif using MAPPIT mutagenesis analysis. Nucleic Acids Res 38: 1902-1912. doi:10.1093/nar/gkp1154. PubMed: 20015971.
59. Huthoff H, Autore F, Gallois-Montbrun S, Fraternali F, Malim MH (2009) RNA-dependent oligomerization of APOBEC3G is required for restriction of HIV-1. PLoS Pathog 5: e1000330. PubMed: 19266078.
60. Zhang K-L, Mangeat B, Ortiz M, Zoete V, Trono D et al. (2007) Model Structure of Human APOBEC3G. PLOS ONE 2: e378. doi:10.1371/journal.pone.0000378. PubMed: 17440614.
61. Shirakawa K, Takaori-Kondo A, Yokoyama M, Izumi T, Matsui M et al. (2008) Phosphorylation of APOBEC3G by protein kinase A regulates its interaction with HIV-1 Vif. Nat Struct Mol Biol 15: 1184-1191. doi:10.1038/nsmb.1497. PubMed: 18836454.
62. Labute P (2008) The generalized Born/volume integral implicit solvent model: estimation of the free energy of hydration using London dispersion instead of atomic surface area. J Comput Chem 29: 1693-1698. doi:10.1002/jcc.20933. PubMed: 18307169.

63. Ponder JW, Case DA (2003) Force fields for protein simulations. Adv Protein Chem 66: 27-85. doi:10.1016/S0065-3233(03)66002-X. PubMed: 14631816.
64. Onufriev A, Bashford D, Case DA (2000) Modification of the Generalized Born Model Suitable for Macromolecules. Journal of Physical Chemistry B 104: 3712-3720. doi:10.1021/jp993855a.
65. Navarro F, Bollman B, Chen H, König R, Yu Q et al. (2005) Complementary function of the two catalytic domains of APOBEC3G. Virology 333: 374-386. doi:10.1016/j.virol.2005.01.011. PubMed: 15721369.
66. Newman EN, Holmes RK, Craig HM, Klein KC, Lingappa JR et al. (2005) Antiviral function of APOBEC3G can be dissociated from cytidine deaminase activity. Curr Biol 15: 166-170. doi:10.1016/j.cub.2004.12.068. PubMed: 15668174.
67. Shandilya SM, Nalam MN, Nalivaika EA, Gross PJ, Valesano JC et al. (2010) Crystal structure of the APOBEC3G catalytic domain reveals potential oligomerization interfaces. Structure 18: 28-38. doi:10.1016/j.str.2009.10.016. PubMed: 20152150.
68. Cho K-i, Kim D, Lee D (2009) A feature-based approach to modeling protein–protein interaction hot spots. Nucleic Acids Res 37: 2672-2687. doi:10.1093/nar/gkp132. PubMed: 19273533.
69. Iwatani Y, Chan DS, Wang F, Maynard KS, Sugiura W et al. (2007) Deaminase-independent inhibition of HIV-1 reverse transcription by APOBEC3G. Nucleic Acids Res 35: 7096-7108. doi:10.1093/nar/gkm750. PubMed: 17942420.
70. Bach D, Peddi S, Mangeat B, Lakkaraju A, Strub K et al. (2008) Characterization of APOBEC3G binding to 7SL RNA. Retrovirology 5: 54. doi:10.1186/1742-4690-5-54. PubMed: 18597676.
71. Muotri AR, Marchetto MC, Coufal NG, Oefner R, Yeo G et al. (2010) L1 retrotransposition in neurons is modulated by MeCP2. Nature 468: 443-446. doi:10.1038/nature09544. PubMed: 21085180.
72. Muotri AR, Chu VT, Marchetto MCN, Deng W, Moran JV et al. (2005) Somatic mosaicism in neuronal precursor cells mediated by L1 retrotransposition. Nature 435: 903-910. doi:10.1038/nature03663. PubMed: 15959507.
73. Tchénio T, Casella JF, Heidmann T (2000) Members of the SRY family regulate the human LINE retrotransposons. Nucleic Acids Res 28: 411-415. doi:10.1093/nar/28.2.411. PubMed: 10606637.
74. Yang N, Kazazian HH Jr. (2006) L1 retrotransposition is suppressed by endogenously encoded small interfering RNAs in human cultured cells. Nat Struct Mol Biol 13: 763-771. doi:10.1038/nsmb1141. PubMed: 16936727.
75. Belancio VP, Roy-Engel AM, Pochampally RR, Deininger P (2010) Somatic expression of LINE-1 elements in human tissues. Nucleic Acids Res 38: 3909-3922. doi:10.1093/nar/gkq132. PubMed: 20215437.
76. Gasior SL, Wakeman TP, Xu B, Deininger PL (2006) The human LINE-1 retrotransposon creates DNA double-strand breaks. J Mol Biol 357: 1383-1393. doi:10.1016/j.jmb.2006.01.089. PubMed: 16490214.
77. Zheng YH, Jeang KT, Tokunaga K (2012) Host restriction factors in retroviral infection: promises in virus-host interaction. Retrovirology 9: 112. doi:10.1186/1742-4690-9-S2-P112. PubMed: 23254112.
78. Wang X, Han Y, Dang Y, Fu W, Zhou T et al. (2010) Moloney leukemia virus 10 (MOV10) protein inhibits retrovirus replication. J Biol Chem 285: 14346-14355. doi:10.1074/jbc.M110.109314. PubMed: 20215113.
79. Furtak V, Mulky A, Rawlings SA, Kozhaya L, Lee K et al. (2010) Perturbation of the P-body component Mov10 inhibits HIV-1 infectivity. PLOS ONE 5: e9081. doi:10.1371/journal.pone.0009081. PubMed: 20140200.
80. Lu C, Luo Z, Jäger S, Krogan NJ, Peterlin BM (2012) Moloney leukemia virus type 10 inhibits reverse transcription and retrotransposition of intracisternal a particles. J Virol 86: 10517-10523. doi:10.1128/JVI.00868-12. PubMed: 22811528.
81. Goodier JL, Cheung LE, Kazazian HH Jr. (2012) MOV10 RNA helicase is a potent inhibitor of retrotransposition in cells. PLoS Genet 8: e1002941. PubMed: 23093941.
82. Arjan-Odedra S, Swanson CM, Sherer NM, Wolinsky SM, Malim MH (2012) Endogenous MOV10 inhibits the retrotransposition of endogenous retroelements but not the replication of exogenous retroviruses. Retrovirology 9: 53. doi:10.1186/1742-4690-9-53. PubMed: 22727223.
83. Gallois-Montbrun S, Kramer B, Swanson CM, Byers H, Lynham S et al. (2007) Antiviral protein APOBEC3G localizes to ribonucleoprotein complexes found in P bodies and stress granules. J Virol 81: 2165-2178. doi:10.1128/JVI.02287-06. PubMed: 17166910.

OPEN ACCESS Freely available online

PLOS ONE

Moderate Restriction of Macrophage-Tropic Human Immunodeficiency Virus Type 1 by SAMHD1 in Monocyte-Derived Macrophages

Kahoru Taya, Emi E. Nakayama, Tatsuo Shioda*

Department of Viral Infections, Research Institute for Microbial Diseases, Osaka University, Suita, Osaka, Japan

Abstract

Macrophage-tropic human immunodeficiency virus type 1 (HIV-1) strains are able to grow to high titers in human monocyte-derived macrophages. However, it was recently reported that cellular protein SAMHD1 restricts HIV-1 replication in human cells of the myeloid lineage, including monocyte-derived macrophages. Here we show that degradation of SAMHD1 in monocyte-derived macrophages was associated with moderately enhanced growth of the macrophage-tropic HIV-1 strain. SAMHD1 degradation was induced by treating target macrophages with vesicular stomatitis virus glycoprotein-pseudotyped human immunodeficiency virus type 2 (HIV-2) particles containing viral protein X. For undifferentiated monocytes, HIV-2 particle treatment allowed undifferentiated monocytes to be fully permissive for productive infection by the macrophage-tropic HIV-1 strain. In contrast, untreated monocytes were totally resistant to HIV-1 replication. These results indicated that SAMHD1 moderately restricts even a macrophage-tropic HIV-1 strain in monocyte-derived macrophages, whereas the protein potently restricts HIV-1 replication in undifferentiated monocytes.

Citation: Taya K, Nakayama EE, Shioda T (2014) Moderate Restriction of Macrophage-Tropic Human Immunodeficiency Virus Type 1 by SAMHD1 in Monocyte-Derived Macrophages. PLoS ONE 9(3): e90969. doi:10.1371/journal.pone.0090969

Editor: Chen Liang, Lady Davis Institute for Medical Research, Canada

Received October 8, 2013; **Accepted** February 5, 2014; **Published** March 5, 2014

Funding: This work was supported by a grant from the Ministry of Education, Culture, Sports, Science, and Technology, and by a grant from the Ministry of Health, Labour and Welfare, Japan. The funders had no role in study design, data collection and analysis, decision to publish, or preparation of the manuscript.

Competing Interests: The authors have declared that no competing interests exist.

* E-mail: shioda@biken.osaka-u.ac.jp

Introduction

CD4 is the primary receptor molecule of human immunodeficiency virus type 1 (HIV-1) for viral attachment to the target cells [1]. HIV-1 thus replicates in $CD4^+$ cells such as activated human $CD4^+$ lymphocytes and macrophages [2,3]. Among different HIV-1 strains, macrophage-tropic HIV-1 strains replicate particularly well in cultured human monocyte-derived macrophages [4]. Many macrophage-tropic HIV-1 strains fail to replicate well in established human T cell lines such as Hut78 and MT4, cell lines in which laboratory-adapted T-cell line-tropic HIV-1 strains can replicate efficiently. Conversely, many laboratory-adapted T-cell line-tropic HIV-1 strains fail to replicate well in monocyte-derived macrophages [5]. Sequence variations in the HIV-1 envelope protein, especially in the third variable region, correlate with the HIV-1 cellular host range [6–9], and this observation led to the identification of the CCR5 and CXCR4 chemokine receptors as HIV-1 co-receptors for viral fusion with target cell membranes [10–16]. Macrophage-tropic HIV-1 strains utilize CCR5 as a co-receptor, and most such macrophage-tropic HIV-1 strains now have been re-designated as R5-tropic strains, although not all the R5-tropic HIV-1 strains can efficiently replicate in macrophages [17–19]. Laboratory-adapted T-cell line-tropic HIV-1 strains utilize CXCR4 as a co-receptor, and most such T-cell line-tropic HIV-1 strains now have been re-designated as X4-tropic strains, although CXCR4 expression also was observed in macrophages [20–22], cells in which X4-tropic strains cannot replicate well.

Despite the presence of the aforementioned HIV-1 strains that can replicate well in macrophages, it has been also reported that HIV-1-based lentivirus vectors composed of HIV-1 Gag and Pol proteins and vesicular stomatitis virus glycoprotein (VSV-G) showed markedly reduced efficiency for transduction of cells of myeloid lineage [23,24]. The restriction was rather strong in monocyte-derived dendritic cells and to a lesser extent in monocyte-derived macrophages [25,26]. Such a myeloid lineage-specific restriction was not observed in lentivirus vectors based on simian immunodeficiency virus isolated from macaques (SIVmac) [26], which is in the same lineage as human immunodeficiency virus type 2 (HIV-2), or in simian immunodeficiency virus isolated from sooty mangabey (SIVsm). The myeloid lineage-specific restriction of HIV-1-based lentivirus vector could also be abrogated by pretreatment of cells with SIVmac particles [27]. Members of HIV-2 and SIVsm lineage encode a non-structural viral protein X (Vpx) that is absent from HIV-1. VpX was shown to abrogate the myeloid lineage-specific restriction of HIV-1-basesd lentivirus vectors [27–29].

In 2011, SAMHD1 (a cellular protein SAM- and HD-domain-containing protein) was implicated as a target of Vpx that was responsible for abrogation of HIV-1 restriction in human cells of myeloid lineage [30,31]. Subsequently, SAMHD1 was shown to restrict HIV-1 infection in resting $CD4^+$ T cells [32]. SAMHD1 possesses deoxynucleoside triphosphate triphosphohydrolase activity; this activity reduces levels of deoxynucleoside triphosphate in cells of myeloid lineage and resting $CD4^+$ cells, thereby preventing reverse-transcription of HIV-1 RNA in these cell types

[33,34]. Vpx antagonizes SAMHD1 and induces proteolytic degradation of SAMHD1 through the CUL4A/DCAF1 E3 ubiquitin ligase complex [30].

In most of the SAMHD1 studies cited above, the efficiency of HIV-1 infection was assayed in the context of lentivirus vectors composed of HIV-1 Gag and Pol proteins packaged with VSV-G protein, along with reporter genes such as those encoding luciferase or green fluorescent protein. This distinction raises the question of whether SAMHD1 provides the same function in live HIV-1 viruses. Therefore, in the study presented here, we re-evaluated the role of SAMHD1 in HIV-1 replication in monocyte-derived macrophages in the context of a live macrophage-tropic HIV-1 strain that can replicate well in macrophages.

Results

Lack of Enhancing Effect of Macrophage-tropic HIV-1 Strain on HIV-1 Infection in Monocyte-derived Macrophages

SAMHD1 was reported to suppress infection of HIV-1-based lentivirus vectors containing VSV-G in cultured monocyte-derived macrophages [30]. On the other hand, macrophage-tropic HIV-1 strains can efficiently replicate in monocyte-derived macrophages [4]. To reconcile these potentially contradictory results, we tested the hypothesis that live macrophage-tropic HIV-1 strains can evade restriction of SAMHD1 by an unidentified mechanism. As a first step, we treated monocyte-derived macrophages with a macrophage-tropic HIV-1 strain SF162 before inoculation with VSV-G-pseudotyped lentivirus vector expressing luciferase (NL43-Luci/VSV-G). Results showed that pretreatment with SF162 failed to enhance subsequent infection by NL43-Luci/VSV-G in macrophages (Fig. 1A and 1B, left panels), whereas pretreatment with VSV-G-pseudotyped and Env-defective HIV-2 particles containing Vpx (GH123-Nhe/VSV-G) enhanced luciferase expression (Fig. 1A and 1B, left panels), as reported previously [30]. The effect of GH123-Nhe/VSV-G was more prominent in undifferentiated monocytes than in fully differentiated macrophages; a more than 200-fold increase of luciferase activity was observed by pretreatment of monocytes with GH123-Nhe/VSV-G (Fig. 1A and 1B, right panels). SF162 again failed to enhance subsequent infection by NL43-Luci/VSV-G in monocytes (Fig. 1A and 1B, right panels).

Enhancing Effect of VSV-G Pseudotyped HIV-2 Particles on Macrophage-tropic HIV-1 Strain in Monocyte-derived Macrophages

We next tested whether GH123-Nhe/VSV-G also could enhance replication of a macrophage-tropic HIV-1 strain in monocyte-derived macrophages. Fig. 2 shows the effects of GH123-Nhe/VSV-G on replication of SF162 in cultured macrophages that were differentiated from monocytes with granulocyte-macrophage colony stimulating factor (GM-CSF). SF162 replicated to titers corresponding to approximately 100 ng/ml of p24 core protein (Fig. 2A and 2B, left panels). Up to five-fold higher titers were detected in SF162-infected macrophages pretreated with GH123-Nhe/VSV-G (Fig. 2A and 2B, left panels). These results indicated that GH123-Nhe/VSV-G could enhance replication of macrophage-tropic HIV-1 in GM-CSF-differentiated macrophage cultures. In contrast, the T-cell line-tropic HIV-1 strain NL43 did not replicate at all in macrophages, regardless of the presence or absence of GH123-Nhe/VSV-G treatment (Fig. 2A and B, right panels).

Monocyte-derived macrophages differentiated with macrophage colony stimulating factor (M-CSF) are more susceptible to HIV-1 infection than those differentiated with GM-CSF [35–38]. We therefore tested whether GH123-Nhe/VSV-G could enhance SF162 replication in monocyte-derived macrophages differentiated with M-CSF. SF162 grew to titers corresponding to 200 ng/ml of p24 in donor 1 macrophages (Fig. 3A, left) and to 400 ng/ml of p24 in donor 2 macrophages (Fig. 3B, left), a level at least two-fold higher than those found in SF162-infected macrophage cultures differentiated with GM-CSF. Up to five-fold higher titers of SF162 also were detected in M-CSF-differentiated macrophage cultures pretreated with GH123-Nhe/VSV-G (Fig. 3A and 3B, left panels). These results indicated that GH123-Nhe/VSV-G could enhance replication of macrophage-tropic HIV-1 replication even in M-CSF-differentiated macrophages. The T-cell line-tropic NL43 strain again did not replicate at all in M-CSF-differentiated macrophages, regardless of the presence or absence of GH123-Nhe/VSV-G treatment (Fig. 3A and 3B, right panels).

Enhancing Effect of VSV-G-pseudotyped HIV-2 Particles on Macrophage-tropic HIV-1 Strain in Undifferentiated Monocytes

In contrast to differentiated macrophages, undifferentiated monocytes are highly resistant to HIV-1 infection, but treatment with GH123-Nhe/VSV-G greatly enhanced VSV-G-pseudotyped lentivirus vector transduction (Fig. 1A and 1B, right panels). This pattern also was observed for live SF162 infection of undifferentiated monocytes (Fig. 4 and 5). SF162 replication in monocytes was not observed until 12 days after infection, when cell morphology suggested that some of the monocytes in the culture had differentiated into macrophages. On the other hand, GH123-Nhe/VSV-G rendered cultured monocytes fully permissive for SF162 replication (Fig. 4A and 4B, left panels). Up to 50-fold higher titers of SF162 were detected in monocytes treated with GH123-Nhe/VSV-G than in untreated monocytes. Consistently, large multi-nucleated syncytia were observed 6 days after infection, but only in monocytes treated with GH123-Nhe/VSV-G (Fig. 5). These results are in good agreement with recent findings that non-stimulated $CD14^+$ cells obtained from Aicardi-Goutieres syndrome patients (who are homozygous for a nonsense mutation in the SAMHD1-encoding gene) were highly susceptible to macrophage-tropic HIV-1 infection [39]. As with GM-CSF- and M-CSF-differentiated macrophages, the T-cell line-tropic NL43 strain did not replicate at all in undifferentiated monocytes, regardless of the presence or absence of GH123-Nhe/VSV-G treatment (Fig. 4A and 4B, right panels).

Levels of SAMHD1 Expression in Monocytes and Macrophages

Vpx was reported to induce proteolytic degradation of SAMHD1. We therefore compared levels of SAMHD1 protein expression in cells treated with GH123-Nhe/VSV-G and those without treatment. As shown in Fig. 6, GH123-Nhe/VSV-G markedly reduced levels of SAMHD1 protein expression in monocytes and macrophages. Consistent with the previous observation [31], levels of SAMHD1 protein expression were apparently higher in undifferentiated monocytes than in macrophages.

We then quantitated levels of SAMHD1 mRNA expression in monocytes and macrophages. As expected, SAMHD1 mRNA levels were higher in monocytes than in macrophages (Fig. 7). There was no difference in SAMHD1 mRNA levels between cells treated with GH123-Nhe/VSV-G and those without treatment.

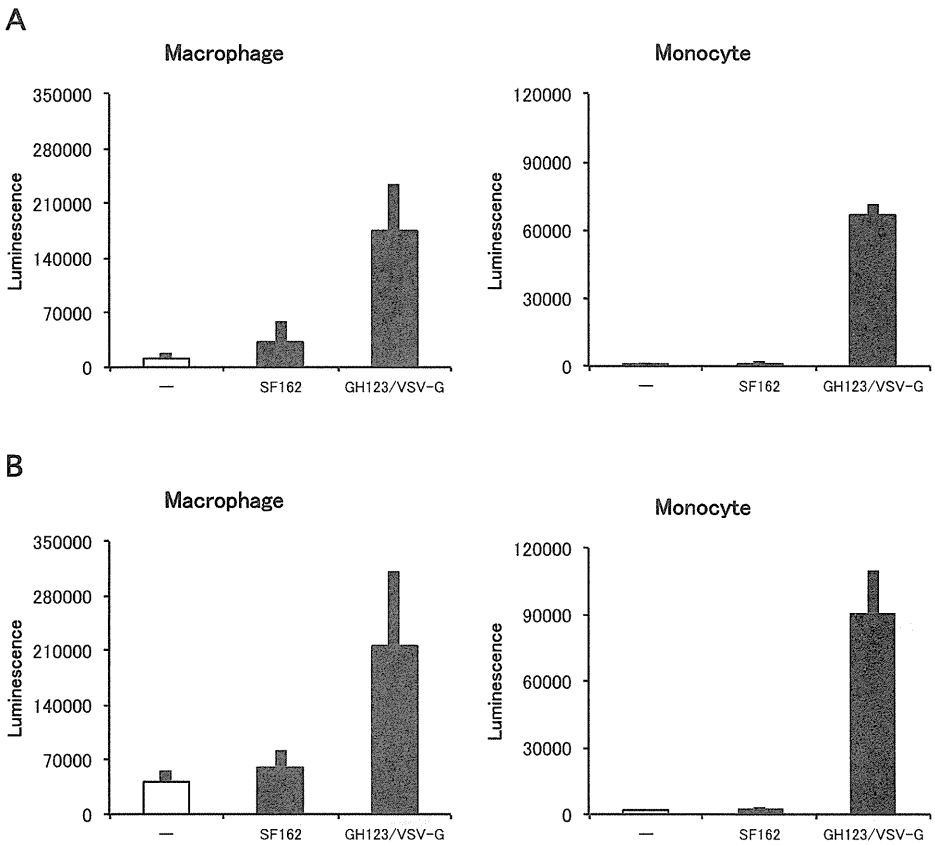

Figure 1. Effects of macrophage-tropic HIV-1 strain and VSV-G-pseudotyped HIV-2 particles on lentivirus vector infection. Monocytes were differentiated into macrophages for 11 days in the presence of GM-CSF. Macrophages or monocytes were treated with macrophage-tropic HIV-1 strain (SF162) or VSV-G pseudotyped and Env-defective HIV-2 particles (GH123/VSV-G) and then infected with lentivirus vector NL43-Luci/VSV-G. Luciferase activity was measured 4 days after infection. Data are plotted as the mean ± SD of triplicate samples; presented data are representative of three independent experiments using two donors. A: Results of samples obtained from a donor 1. B: Results of samples obtained from a donor 2.
doi:10.1371/journal.pone.0090969.g001

These results confirmed that reduced SAMHD1 protein levels in cells treated with GH123-Nhe/VSV-G were caused by enhanced degradation of SAMHD1 by HIV-2 particles containing Vpx.

Phosphorylation of SAMHD1 in Monocytes and Differentiated Macrophages

It was recently reported that Cyclin A2/CDK1 phosphorylates SAMHD1 at the threonine 592 residues. Phosphorylation of the SAMHD1 threonine 592 correlates with loss of its ability to restrict HIV-1 [40–42]. We therefore analyzed the phosphorylation state of SAMHD1 in monocytes and differentiated macrophages. As shown in Fig. 8, SAMHD1 proteins in monocytes were less phosphorylated than those in GM-CSF-differentiated or M-CSF-differentiated macrophages. This result is in good agreement with those reported previously [40], and correlated well with our results that SAMHD1 restriction in monocytes was much more potent than that in differentiated macrophages (Fig. 1 and 4). Treatment with GH123-Nhe/VSV-G reduced both phosphorylated and nonphosphorylated SAMHD1 in all cells. There was no difference in the phosphorylation state of SAMHD1 between GM-CSF-differentiated and M-CSF-differentiated macrophages (Fig. 8).

Enhancing Effect of SAMHD1 siRNA on HIV-1 Infection in Monocytes and Monocyte-derived Macrophages

To confirm that the observed enhancing effect of VSV-G-pseudotyped HIV-2 particles on HIV-1 infection was due to degradation of SAMHD1 in monocytes and macrophages, we used siRNAs targeting SAMHD1 to reduce levels of SAMHD1 expression. The siRNAs targeting SAMHD1 reduced levels of SAMHD1 mRNA in both monocytes and GM-CSF-differentiated macrophages (Fig. 9A and 9B, left panels). Accordingly, increased levels of NL43-Luci/VSV-G infection were observed in monocytes (Fig. 9A and 9B, middle panels) and GM-CSF-differentiated macrophages (Fig. 9A and 9B, right panels) transfected with the siRNAs targeting SAMHD1. These results confirmed that the enhancing effect of VSV-G-pseudotyped HIV-2 particles on HIV-1 infection was due to degradation of SAMHD1.

Discussion

SAMHD1 was reported to suppress HIV-1 infection of cells of myeloid lineage, including monocyte-derived macrophages [30,31]. Nevertheless, macrophage-tropic HIV-1 strains can efficiently replicate in monocyte-derived macrophages [4,6–8].

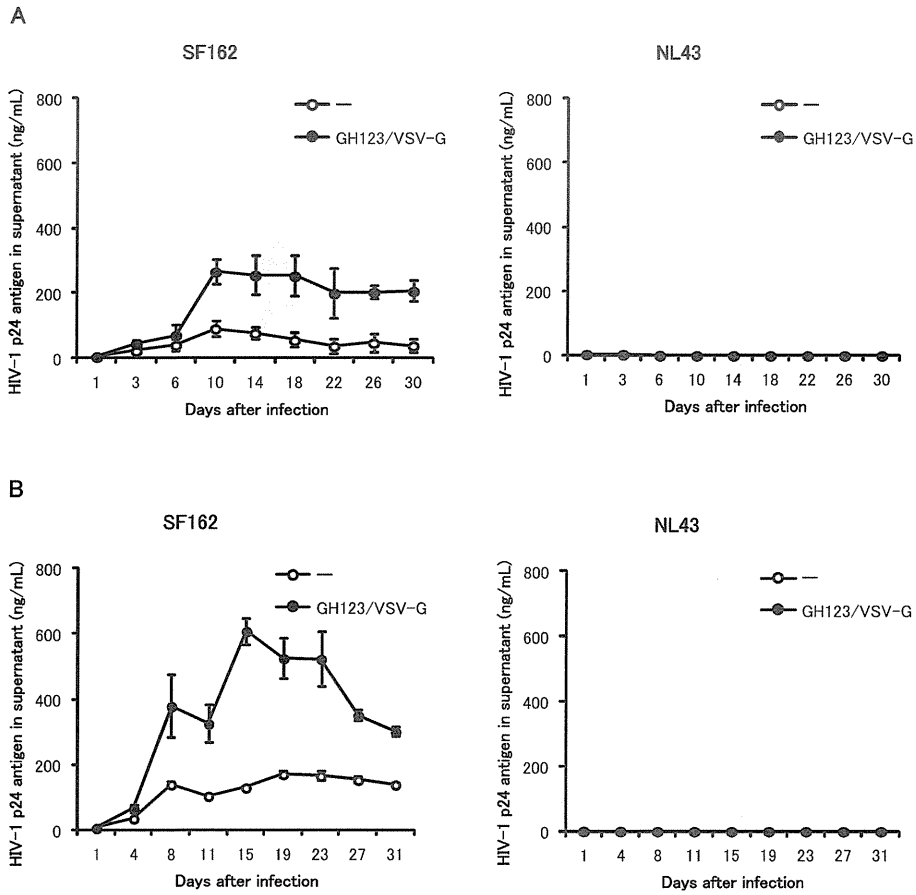

Figure 2. Effects of VSV-G-pseudotyped HIV-2 particles on macrophage-tropic and T-cell line-tropic HIV-1 strains in GM-CSF-induced macrophages. Monocytes were differentiated into macrophages for 6 days in the presence of GM-CSF. Macrophages were treated with VSV-G pseudotyped and Env-defective HIV-2 particles (GH123/VSV-G) and then infected with HIV-1 strain SF162 or NL43. HIV-1 replication was quantified by ELISA measurement of p24 antigen in the supernatant after infection. Data are plotted as the mean ± SD of triplicate samples; presented data are representative of three independent experiments using two donors. A: Results of samples obtained from a donor 1. B: Results of samples obtained from a donor 2.
doi:10.1371/journal.pone.0090969.g002

In the present study, we have shown that the treatment of monocyte-derived macrophages or undifferentiated monocytes with GH123-Nhe/VSV-G enhanced subsequent macrophage-tropic HIV-1 infection. GH123-Nhe/VSV-G treatment reduced levels of SAMHD1 protein expression in monocyte-derived macrophages and undifferentiated monocytes. Enhancing effects by GH123-Nhe/VSV-G were observed even in M-CSF-induced monocyte-derived macrophages, which were reported to be highly susceptible to HIV-1 infection [35–38,43]. These results indicated that SAMHD1 could moderately suppress replication of the macrophage-tropic HIV-1 strain in monocyte-derived macrophages. It is formally possible that live macrophage-tropic HIV-1 strains evade restriction of SAMHD1 by an unidentified mechanism, although we consider such a possibility unlikely.

Levels of HIV-1 restriction by SAMHD1 in monocyte-derived macrophages were rather modest, while those in undifferentiated monocytes were quite strong (Fig. 2, 3 and 4). SAMHD1 expression levels were higher in undifferentiated monocytes than in monocyte-derived macrophages (Fig. 6 and 7), showing a clear correlation between levels of SAMHD1 expression and those of restriction. Furthermore, phosphorylation of SAMHD1, which was reported to abolish HIV-1 restriction activity of SAMHD1 [40–42], was more prominent in M-CSF-induced or GM-CSF-induced macrophages than in undifferentiated monocytes (Fig. 8). When we compared M-CSF-induced and GM-CSF-induced macrophages, HIV-1 grew to higher titers in M-CSF-induced macrophages than in GM-CSF-induced macrophages. This result is in good agreement with those of the previous studies [37,43]. The levels of restriction by SAMHD1 also were slightly lower in M-CSF-induced macrophages than in GM-CSF-induced macrophages, although we failed to observe clear differences in levels of expression or phosphorylation state of SAMHD1 between M-CSF-induced and GM-CSF-induced macrophages (Fig. 6, 7, and 8). Thus, mechanisms underlying the higher sensitivity to HIV-1 infection in M-CSF-induced macrophages are not clear at present; further studies are necessary, including comparisons of CD4 and CCR5 expression levels between M-CSF-induced and GM-CSF-induced macrophages.

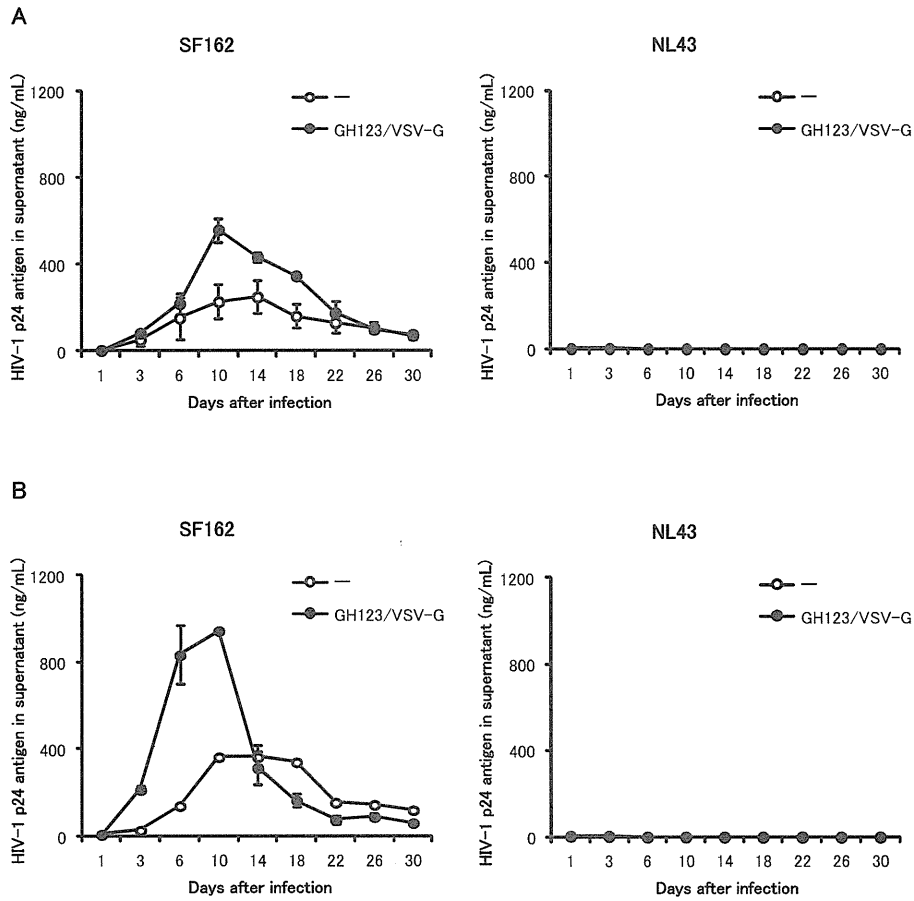

Figure 3. Effects of VSV-G-pseudotyped HIV-2 particles on macrophage-tropic and T-cell line-tropic HIV-1 strains in M-CSF-induced macrophages. Monocytes were differentiated into macrophages for 6 days in the presence of M-CSF. Macrophages were treated with VSV-G pseudotyped and Env-defective HIV-2 particles (GH123/VSV-G) and then infected with HIV-1 strain SF162 or NL43. HIV-1 replication was quantified by ELISA measurement of p24 antigen in the supernatant after infection. Data are plotted as the mean ± SD of triplicate samples; presented data are representative of two independent experiments using two donors. A: Results of samples obtained from a donor 1. B: Results of samples obtained from a donor 2.
doi:10.1371/journal.pone.0090969.g003

It should be noted here that the effects of GH123-Nhe/VSV-G treatment seem to last relatively long, although we treated cells only once with GH123-Nhe/VSV-G. It is possible that the Vpx protein produced by the transduced HIV-2 genomes was incorporated into infectious SF162 progeny virions and thus facilitated replication of SF162 in the next cycle of infection. It is also possible that Env-deficient progeny HIV-2 virions were pseudotyped with fully functional SF162 envelope proteins, and thereby continued to produce Vpx that degraded SAMHD1.

Similar to monocytes and macrophages, microglial cells in the human brain are derived via the myeloid lineage and are also susceptible to HIV-1 infection [44]. HIV-1-infected microglial cells appear to play an important role in HIV-1-associated neurological disorders such as dementia and neurocognitive disorder [45]. It therefore would be interesting to investigate whether or not SAMHD1 moderately suppresses HIV-1 replication in microglial cells just as in macrophages. If SAMHD1 can suppress HIV-1 replication at least moderately in microglial cells, artificial potentiation of SAMHD1 in microglial cells might be a novel approach to the treatment of HIV-1-associated neurological disorders.

In conclusion, we have shown that SAMHD1 moderately restricts even macrophage-tropic HIV-1 strains in monocyte-derived macrophages. SAMHD1 restriction was much more potent in undifferentiated monocytes than that in GM-CSF-differentiated or M-CSF-differentiated macrophages. Levels of expression and phosphorylation state of SAMHD1 could at least partially explain the different levels of SAMHD1 restriction between undifferentiated monocytes and differentiated macrophages.

Materials and Methods

Ethics Statement

Peripheral blood mononuclear cells (PBMC) were obtained from healthy donors with written informed consent. Use of human

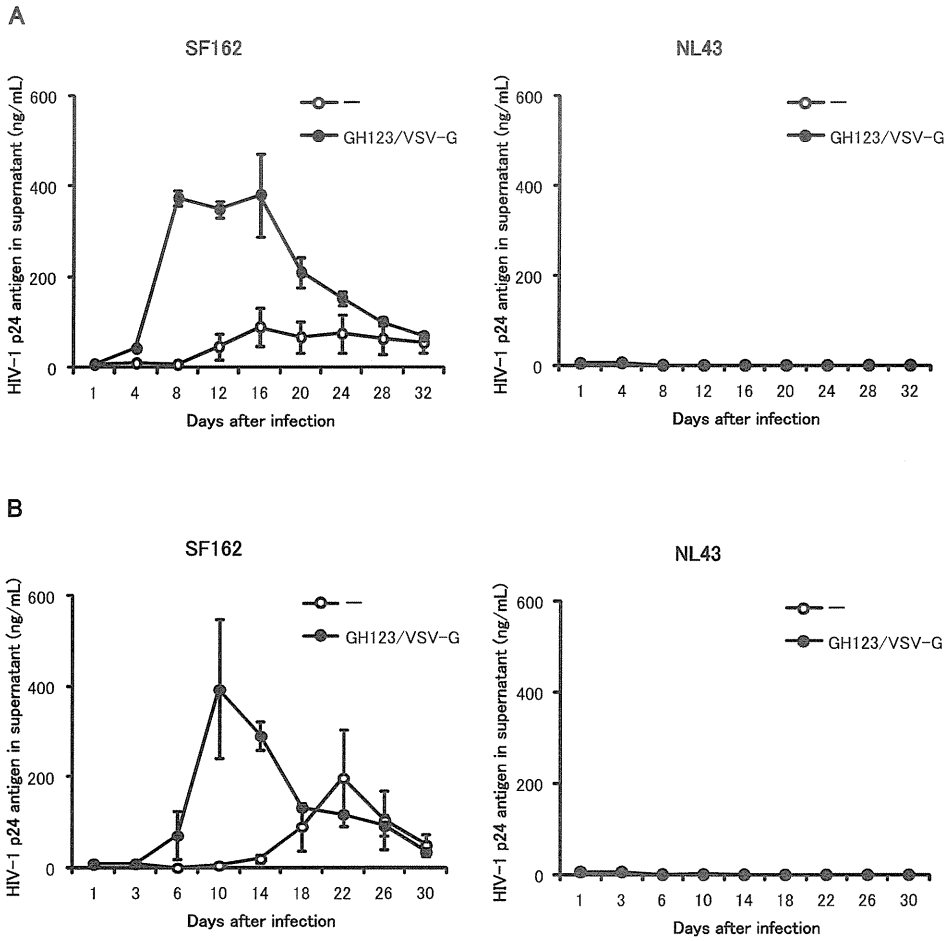

Figure 4. Effects of VSV-G-pseudotyped HIV-2 particles on macrophage-tropic and T-cell line-tropic HIV-1 strains in undifferentiated monocytes. Monocytes were treated with VSV-G pseudotyped and Env-defective HIV-2 particles (GH123/VSV-G) and then infected with HIV-1 strain SF162 or NL43. HIV-1 replication was quantified by ELISA measurement of p24 antigen in the supernatant after infection. Data are plotted as the mean ± SD of triplicate samples obtained from a single blood donor; presented data are representative of three independent experiments using two donors. A: Results of samples obtained from a donor 1. B: Results of samples obtained from a donor 2.
doi:10.1371/journal.pone.0090969.g004

materials in this study was approved by the Research Ethics Committee of Osaka University.

Viruses

Macrophage-tropic HIV-1 strain SF162 and laboratory-adapted T-cell line-tropic HIV-1 strain NL43 were grown in CCR5-expressing MT4 cells [46] and titrated for use with the RETROtek Antigen ELISA kit (ZeptoMetrix, Buffalo, NY). VSV-G-pseudotyped lentivirus vector expressing luciferase (NL43-Luci/VSV-G) and VSV-G-pseudotyped and Env-defective HIV-2 particles containing Vpx (GH123-Nhe/VSV-G) were produced from human embryonic kidney cells (293T cells) using polyethylenimine (PEI) (molecular weight, 25,000; Polysciences, Warrington, PA). Briefly, for NL43-Luci/VSV-G virus production, 293T cells were transfected with 15 μg of pNL4-3-Luc-R-E- plasmid and 5 μg of VSV-G-encoding plasmid; for GH123-Nhe/VSV-G virus production, 293T cells were transfected with 15 μg of GH123-Nhe and 5 μg of VSV-G-encoding plasmid. The GH123-Nhe plasmid was generated by blunting the *Nhe*I site in the HIV-2 GH123 plasmid, thereby introducing a frame-shift mutation in its *env* gene. For transfected cells, medium was replaced 6 h after transfection, and viruses were harvested 48 h later. Viral titers were measured with the RETROtek Antigen ELISA kit.

Cells

PBMCs were obtained from blood buffy coats of healthy donors using Ficoll-Paque density gradient centrifugation, and then plated in 24-well, 12-well, or 6-well MULTIWELL PRIMARIA plates (Becton Dickinson, Franklin Lakes, NJ) with RPMI 1640 supplemented with 10% fetal calf serum (FCS). To obtain the monocyte population, the floating cells were removed by washing the plates with phosphate-buffered saline (PBS) four times after incubation at 37°C for 1 day. Monocytes were differentiated into macrophages for 6–11 days in the presence of 100 ng/ml of granulocyte macrophage colony stimulating factor (GM-CSF)

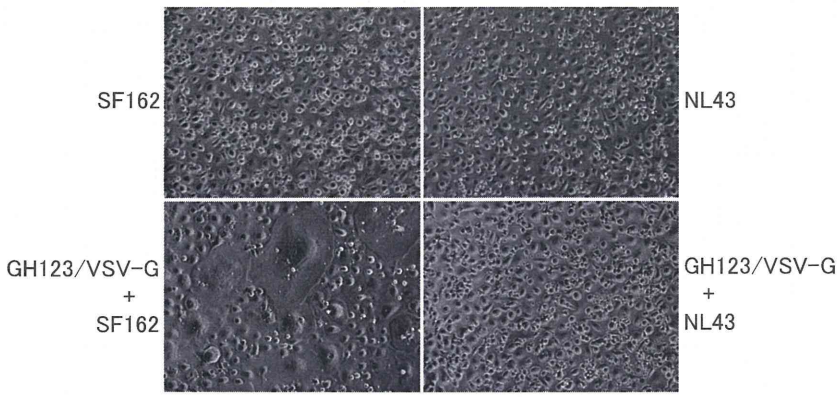

Figure 5. Syncytium formation in undifferentiated monocytes pretreated with HIV-2 particles and then infected with macrophage-tropic HIV-1. Monocytes were treated with VSV-G pseudotyped and Env-defective HIV-2 particles (GH123/VSV-G) and then infected with HIV-1 strain SF162 or NL43. Presented data are representative of two independent experiments.
doi:10.1371/journal.pone.0090969.g005

(PeproTECH, Rocky Hill, NJ) or 100 ng/ml of macrophage colony stimulating factor (M-CSF) (PeproTECH).

Luciferase Assay

Macrophages ($1.6–2.4\times10^5$ cells) and monocytes ($2.6–3.4\times10^6$ cells) were pretreated for 2 h with a titer of macrophage-tropic HIV-1 strain SF162 virus equivalent to 100 ng of p24 or with a titer of GH123-Nhe/VSV-G virus equivalent to 100 ng of p27, and then infected with a titer of NL43-Luci/VSV-G virus equivalent to 7.7 ng of p24. After incubation for 2 h, the medium was changed, and cells were incubated for 4 days at 37°C. Luciferase activity was measured in cell lysates according to the manufacturer's instructions (Bright-Glo Luciferase Assay System, Promega, Madison, WI) and read using a Centro LB960 Microplate Luminometer (Berthold, Bad Wildbad, Germany).

Virus Infection

Macrophages and monocytes ($2.2–2.6\times10^6$ cells) were pretreated for 2 h with a titer of GH123-Nhe/VSV-G virus equivalent to 100 ng of p27, and then infected with a titer of virus equivalent to 100 ng of p24 of macrophage-tropic HIV-1 strain SF162 or laboratory-adapted T-cell line-tropic HIV-1 strain NL43. After incubation for 2 h, cells were washed with PBS and incubated with RPMI 1640 supplemented with 10% FCS and 100 ng/ml GM-CSF or 100 ng/ml M-CSF. Culture supernatants were collected periodically, and levels of HIV-1 p24 antigen were measured by the RETROtek HIV-1 p24 Antigen ELISA kit.

Western Blot

Monocytes and macrophages (3.5×10^6 cells) were lysed in Laemmli sample buffer (100 mM Tris-HCl, pH 6.8, 0.04% sodium dodecyl sulfate (SDS), 20% glycerol, 0.12% 2-mercaptoethanol). Proteins in the lysates were subjected to SDS-polyacrylamide gel electrophoresis (SDS-PAGE). Proteins in the gel were

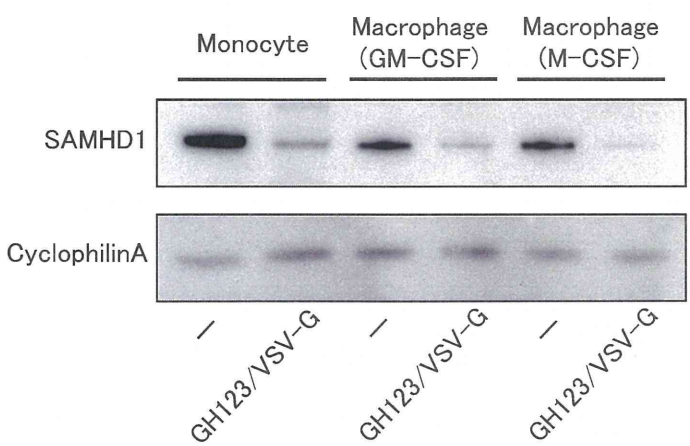

Figure 6. Western blot analysis of SAMHD1 in undifferentiated monocytes and macrophages. Monocytes were differentiated into macrophages for 6 days in the presence of GM-CSF or M-CSF. Macrophages or monocytes were treated with or without VSV-G-pseudotyped and Env-defective HIV-2 particles (GH123/VSV-G), and harvested. Whole-cell extracts were separated on SDS-PAGE and analyzed by western blot using the indicated antibodies. Presented data are representative of two independent experiments.
doi:10.1371/journal.pone.0090969.g006

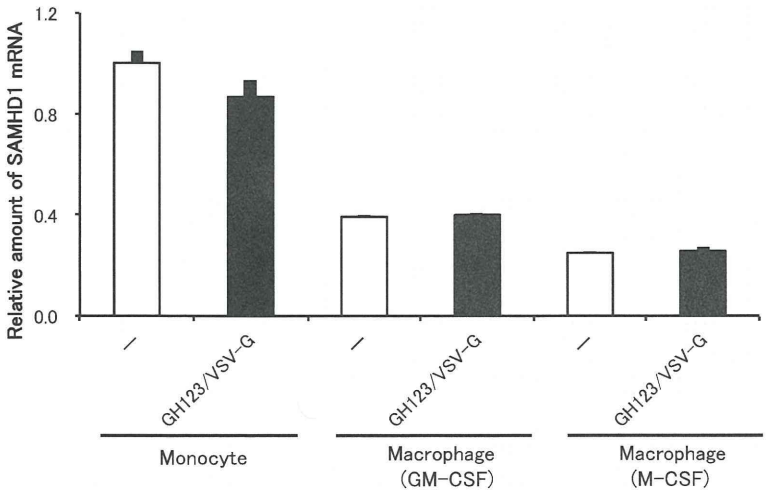

Figure 7. Quantification of SAMHD1 mRNA expression. Monocytes were differentiated into macrophages for 6 days in the presence of GM-CSF or M-CSF. Macrophages or monocytes were treated with or without VSV-G-pseudotyped and Env-defective HIV-2 particles (GH123/VSV-G), and harvested. SAMHD1 mRNA expression levels were detected by real-time RT-PCR and normalized against GAPDH. Data are shown as mean ± SD.
doi:10.1371/journal.pone.0090969.g007

then electrically transferred to a membrane (Immobilion; Millipore, Billerica, MA). Blots were blocked and probed with anti-CypA affinity rabbit polyclonal antibody (Sigma, St. Louis, MO) overnight at 4°C. Blots then were incubated with peroxidase-linked protein A (GE Healthcare, Buckinghamshire, UK), and bound antibodies were visualized with a Chemilumi-One chemiluminescent kit (Nacalai Tesque, Kyoto, Japan). Quantities of cell lysate were normalized by CypA level, then subjected to a new round of SDS-PAGE and membrane transfer. For the new blot, SAMHD1 protein in the membrane was detected with anti-SAMHD1 (611–625) rabbit antibody (Sigma) followed by peroxidase-linked protein A (GE Healthcare, Buckinghamshire, UK) detection as described above.

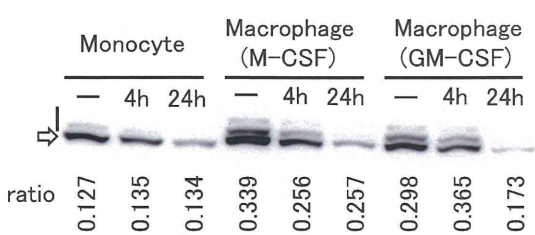

Figure 8. Phosphorylation state of SAMHD1. Monocytes (Monocyte), M-CSF-differentiated macrophages (Macrophage (M-CSF)), and GM-CSF-differentiated macrophages (Macrophage (GM-CSF)) were treated with GH123-Nhe/VSV-G for 2 h and incubated at 37°C for 4 h (4 h) or 24 h (24 h), or mock-treated (−). Cells were lyzed and subjected for SDS-PAGE containing Phos-tag to separate phosphorylated proteins from nonphosphorylated ones. SAMHD1 proteins were detected by anti-SAMHD1 antibody. Upper bands shown by a vertical bar and a lower band shown by an arrow represent phosphorylated and nonphosphorylated SAMHD1, respectively. Ratios of phosphorylated SAMHD1 levels to total SAMHD1 levels (ratio) are shown in vertical numbers.
doi:10.1371/journal.pone.0090969.g008

Phosphorylation State of SAMHD1

Monocyte or macrophages (6×10^6 cells) were treated with a titer of GH123-Nhe/VSV-G virus equivalent to 500 ng of p25 for 2 h, washed with medium, and then incubated at 37°C for 4 h or 24 h. Cells were lysed in Laemmli sample buffer. Proteins in the lysates were separated by SDS-PAGE containing Phos-tag (Wako, Osaka, Japan), a ligand that decreases the mobility of phosphorylated proteins. Separated proteins in the gel were analyzed by western blotting using anti-SAMHD1 antibody. The gel images were analyzed by CS analyzer 3.0 (ATTO, Tokyo, Japan).

Quantification of SAMHD1 mRNA Expression

Total RNA was extracted from monocytes or macrophages using TRIZOL reagent (Life Technologies, Carlsbad, CA) following the manufacturer's instructions. cDNA was synthesized from 1 μg of total RNA using the High-capacity cDNA Archive kit (Applied Biosystems, Carlsbad, CA) according to the manufacturer's instructions. For real time PCR, each 20-μL reaction mixture consisted of 5 μL of cDNA, 10 μL TaqMan Universal PCR Master Mix (Applied Biosystems, Carlsbad, CA) and 1 μL of TaqMan Gene Ex Assays (Assay ID: Hs00210019_m1). Real time PCR was performed with an Applied Biosystems 7500 Real-Time PCR System. Levels of SAMHD1 mRNA were normalized with those of GAPDH according to the manufacturer's instructions.

RNA Interference

The cultured medium of monocytes ($1.6–2.4\times10^6$ cells) was replaced with 0.5 mL of Opti-MEM (Gibco, Carlsbad, CA) before transfection. The SAMHD1-targeting pool comprised of the siRNAs to the following target sequences: J-013950-09: 5′-GACAAUGAGUUGCGUAUUU-3′; J-013950-10: 5′-CAUGUUUGAUGGACGAUUU-3′; J-013950-11: 5′-AAGUAUUGCUAGACGUGAA-3′; J-013950-12: 5′-UUAGUUAUAUCCAGCGAUU-3′ were purchased from Dharmacon (Lafayette, CO). The GFP-targeting siRNA to the sequence 5′-GGCTACGTCCAGGAGCGCACC-3′ were used as a control siRNA. Monocytes were transfected with 40 pmol aliquots of siRNA with 2 μL of Lipofectamine 2000 (Invitrogen, Carlsbad,

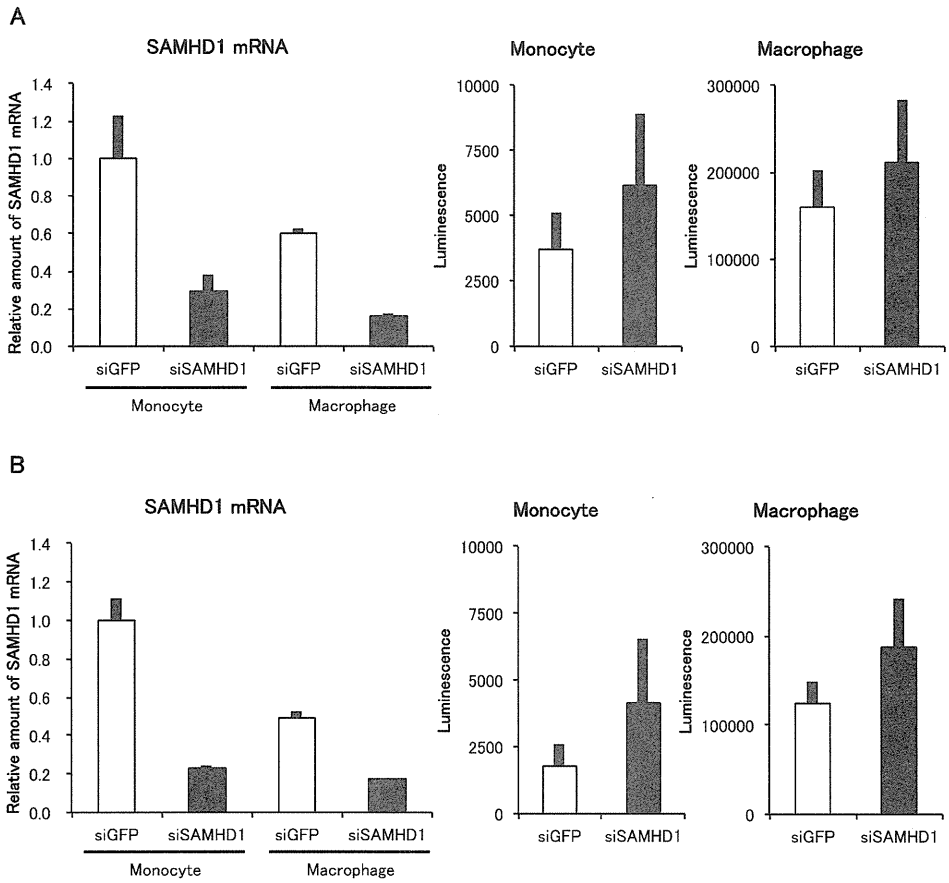

Figure 9. Effects of SAMHD1 siRNA on HIV-1 infection. Monocytes (Monocyte) or macrophages (Macrophage) were treated with SAMHD1- (siSAMHD1) or GFP- (siGFP) targeting siRNAs. Three days after transfection, cells were harvested or infected with NL43-Luci/VSV-G virus. SAMHD1 mRNA expression levels in harvested cells were detected by real-time RT-PCR and normalized against GAPDH. Data are shown as mean ± SD. Luciferase activity in infected cells was measured 4 days after infection. Data are plotted as the mean ± SD of triplicate samples; presented data are representative of two independent experiments using two donors. A: Results of samples obtained from a donor 1. B: Results of samples obtained from a donor 2.
doi:10.1371/journal.pone.0090969.g009

CA) per well. Six h after transfection, cultured medium was replaced with RPMI 1640 supplemented with 10% FCS. At day 3, monocytes were infected with a titer of NL43-Luci/VSV-G virus equivalent to 7.7 ng of p24. In the case of GM-CSF-induced macrophages ($1.6–3.6\times10^6$ cells), siRNAs were transfected at day 4 after differentiation by GM-CSF, and then infected with NL43-Luci/VSV-G virus at day 7. Total RNA was extracted from cells at the time point of NL43-Luci/VSV-G virus infection for quantification of SAMHD1 mRNA expression.

Acknowledgments

We are grateful to Dr. Tetsuro Matano for his critical discussion of this study. We thank Ms. Noriko Teramoto for her assistance. pNL4-3-Luc-R-E- plasmid was obtained through the AIDS Research and Reference Reagent Program, Division of AIDS, NIAID, NIH.

Author Contributions

Conceived and designed the experiments: EEN TS. Performed the experiments: KT EEN. Analyzed the data: KT EEN TS. Wrote the paper: KT EEN TS.

References

1. Maddon PJ, Dalgleish AG, McDougal JS, Clapham PR, Weiss RA, et al. (1986) The T4 gene encodes the AIDS virus receptor and is expressed in the immune system and the brain. Cell 47: 333–348.
2. Gartner S, Markovits P, Markovitz DM, Kaplan MH, Gallo RC, et al. (1986) The role of mononuclear phagocytes in HTLV-III/LAV infection. Science 233: 215–219.
3. Koenig S, Gendelman HE, Orenstein JM, Dal Canto MC, Pezeshkpour GH, et al. (1986) Detection of AIDS virus in macrophages in brain tissue from AIDS patients with encephalopathy. Science 233: 1089–1093.
4. Cheng-Mayer C, Weiss C, Seto D, Levy JA (1989) Isolates of human immunodeficiency virus type 1 from the brain may constitute a special group of the AIDS virus. Proc Natl Acad Sci U S A 86: 8575–8579.
5. Cheng-Mayer C, Seto D, Tateno M, Levy JA (1988) Biologic features of HIV-1 that correlate with virulence in the host. Science 240: 80–82.
6. Hwang SS, Boyle TJ, Lyerly HK, Cullen BR (1991) Identification of the envelope V3 loop as the primary determinant of cell tropism in HIV-1. Science 253: 71–74.

7. O'Brien WA, Koyanagi Y, Namazie A, Zhao JQ, Diagne A, et al. (1990) HIV-1 tropism for mononuclear phagocytes can be determined by regions of gp120 outside the CD4-binding domain. Nature 348: 69–73.
8. Shioda T, Levy JA, Cheng-Mayer C (1991) Macrophage and T cell-line tropisms of HIV-1 are determined by specific regions of the envelope gp120 gene. Nature 349: 167–169.
9. Shioda T, Levy JA, Cheng-Mayer C (1992) Small amino acid changes in the V3 hypervariable region of gp120 can affect the T-cell-line and macrophage tropism of human immunodeficiency virus type 1. Proc Natl Acad Sci U S A 89: 9434–9438.
10. Alkhatib G, Combadiere C, Broder CC, Feng Y, Kennedy PE, et al. (1996) CC CKR5: a RANTES, MIP-1alpha, MIP-1beta receptor as a fusion cofactor for macrophage-tropic HIV-1. Science 272: 1955–1958.
11. Berson JF, Long D, Doranz BJ, Rucker J, Jirik FR, et al. (1996) A seven-transmembrane domain receptor involved in fusion and entry of T-cell-tropic human immunodeficiency virus type 1 strains. J Virol 70: 6288–6295.
12. Choe H, Farzan M, Sun Y, Sullivan N, Rollins B, et al. (1996) The beta-chemokine receptors CCR3 and CCR5 facilitate infection by primary HIV-1 isolates. Cell 85: 1135–1148.
13. Deng H, Liu R, Ellmeier W, Choe S, Unutmaz D, et al. (1996) Identification of a major co-receptor for primary isolates of HIV-1. Nature 381: 661–666.
14. Doranz BJ, Rucker J, Yi Y, Smyth RJ, Samson M, et al. (1996) A dual-tropic primary HIV-1 isolate that uses fusin and the beta-chemokine receptors CKR-5, CKR-3, and CKR-2b as fusion cofactors. Cell 85: 1149–1158.
15. Dragic T, Litwin V, Allaway GP, Martin SR, Huang Y, et al. (1996) HIV-1 entry into CD4+ cells is mediated by the chemokine receptor CC-CKR-5. Nature 381: 667–673.
16. Feng Y, Broder CC, Kennedy PE, Berger EA (1996) HIV-1 entry cofactor: functional cDNA cloning of a seven-transmembrane, G protein-coupled receptor. Science 272: 872–877.
17. Gorry PR, Ancuta P (2011) Coreceptors and HIV-1 pathogenesis. Curr HIV/AIDS Rep 8: 45–53.
18. Peters PJ, Duenas-Decamp MJ, Sullivan WM, Clapham PR (2007) Variation of macrophage tropism among HIV-1 R5 envelopes in brain and other tissues. J Neuroimmune Pharmacol 2: 32–41.
19. Koyanagi Y, Miles S, Mitsuyasu RT, Merrill JE, Vinters HV, et al. (1987) Dual infection of the central nervous system by AIDS viruses with distinct cellular tropisms. Science 236: 819–822.
20. Cashin K, Roche M, Sterjovski J, Ellett A, Gray LR, et al. (2011) Alternative coreceptor requirements for efficient CCR5- and CXCR4-mediated HIV-1 entry into macrophages. J Virol 85: 10699–10709.
21. Lapham CK, Zaitseva MB, Lee S, Romanstseva T, Golding H (1999) Fusion of monocytes and macrophages with HIV-1 correlates with biochemical properties of CXCR4 and CCR5. Nat Med 5: 303–308.
22. Tokunaga K, Greenberg ML, Morse MA, Cumming RI, Lyerly HK, et al. (2001) Molecular basis for cell tropism of CXCR4-dependent human immunodeficiency virus type 1 isolates. J Virol 75: 6776–6785.
23. Gruber A, Kan-Mitchell J, Kuhen KL, Mukai T, Wong-Staal F (2000) Dendritic cells transduced by multiply deleted HIV-1 vectors exhibit normal phenotypes and functions and elicit an HIV-specific cytotoxic T-lymphocyte response in vitro. Blood 96: 1327–1333.
24. Tan PH, Beutelspacher SC, Xue SA, Wang YH, Mitchell P, et al. (2005) Modulation of human dendritic-cell function following transduction with viral vectors: implications for gene therapy. Blood 105: 3824–3832.
25. Kaushik R, Zhu X, Stranska R, Wu Y, Stevenson M (2009) A cellular restriction dictates the permissivity of nondividing monocytes/macrophages to lentivirus and gammaretrovirus infection. Cell Host Microbe 6: 68–80.
26. Negre D, Mangeot PE, Duisit G, Blanchard S, Vidalain PO, et al. (2000) Characterization of novel safe lentiviral vectors derived from simian immunodeficiency virus (SIVmac251) that efficiently transduce mature human dendritic cells. Gene Ther 7: 1613–1623.
27. Goujon C, Jarrosson-Wuilleme L, Bernaud J, Rigal D, Darlix JL, et al. (2006) With a little help from a friend: increasing HIV transduction of monocyte-derived dendritic cells with virion-like particles of SIV(MAC). Gene Ther 13: 991–994.
28. Goujon C, Arfi V, Pertel T, Luban J, Lienard J, et al. (2008) Characterization of simian immunodeficiency virus SIVSM/human immunodeficiency virus type 2 Vpx function in human myeloid cells. J Virol 82: 12335–12345.
29. Goujon C, Riviere L, Jarrosson-Wuilleme L, Bernaud J, Rigal D, et al. (2007) SIVSM/HIV-2 Vpx proteins promote retroviral escape from a proteasome-dependent restriction pathway present in human dendritic cells. Retrovirology 4: 2.
30. Hrecka K, Hao C, Gierszewska M, Swanson SK, Kesik-Brodacka M, et al. (2011) Vpx relieves inhibition of HIV-1 infection of macrophages mediated by the SAMHD1 protein. Nature 474: 658–661.
31. Laguette N, Sobhian B, Casartelli N, Ringeard M, Chable-Bessia C, et al. (2011) SAMHD1 is the dendritic- and myeloid-cell-specific HIV-1 restriction factor counteracted by Vpx. Nature 474: 654–657.
32. Baldauf HM, Pan X, Erikson E, Schmidt S, Daddacha W, et al. (2012) SAMHD1 restricts HIV-1 infection in resting CD4(+) T cells. Nat Med 18: 1682–1687.
33. Goldstone DC, Ennis-Adeniran V, Hedden JJ, Groom HC, Rice GI, et al. (2011) HIV-1 restriction factor SAMHD1 is a deoxynucleoside triphosphate triphosphohydrolase. Nature 480: 379–382.
34. Kim B, Nguyen LA, Daddacha W, Hollenbaugh JA (2012) Tight interplay among SAMHD1 protein level, cellular dNTP levels, and HIV-1 proviral DNA synthesis kinetics in human primary monocyte-derived macrophages. J Biol Chem 287: 21570–21574.
35. Bergamini A, Perno CF, Dini L, Capozzi M, Pesce CD, et al. (1994) Macrophage colony-stimulating factor enhances the susceptibility of macrophages to infection by human immunodeficiency virus and reduces the activity of compounds that inhibit virus binding. Blood 84: 3405–3412.
36. Kedzierska K, Maerz A, Warby T, Jaworowski A, Chan H, et al. (2000) Granulocyte-macrophage colony-stimulating factor inhibits HIV-1 replication in monocyte-derived macrophages. AIDS 14: 1739–1748.
37. Matsuda S, Akagawa K, Honda M, Yokota Y, Takebe Y, et al. (1995) Suppression of HIV replication in human monocyte-derived macrophages induced by granulocyte/macrophage colony-stimulating factor. AIDS Res Hum Retroviruses 11: 1031–1038.
38. Pauls E, Jimenez E, Ruiz A, Permanyer M, Ballana E, et al. (2013) Restriction of HIV-1 replication in primary macrophages by IL-12 and IL-18 through the upregulation of SAMHD1. J Immunol 190: 4736–4741.
39. Berger A, Sommer AF, Zwarg J, Hamdorf M, Welzel K, et al. (2011) SAMHD1-deficient CD14+ cells from individuals with Aicardi-Goutieres syndrome are highly susceptible to HIV-1 infection. PLoS Pathog 7: e1002425.
40. Cribier A, Descours B, Valadao AL, Laguette N, Benkirane M (2013) Phosphorylation of SAMHD1 by cyclin A2/CDK1 regulates its restriction activity toward HIV-1. Cell Rep 3: 1036–1043.
41. White TE, Brandariz-Nunez A, Valle-Casuso JC, Amie S, Nguyen LA, et al. (2013) The retroviral restriction ability of SAMHD1, but not its deoxynucleotide triphosphohydrolase activity, is regulated by phosphorylation. Cell Host Microbe 13: 441–451.
42. Welbourn S, Dutta SM, Semmes OJ, Strebel K (2013) Restriction of virus infection but not catalytic dNTPase activity is regulated by phosphorylation of SAMHD1. J Virol 87: 11516–11524.
43. Diget EA, Zuwala K, Berg RK, Laursen RR, Soby S, et al. (2013) Characterization of HIV-1 infection and innate sensing in different types of primary human monocyte-derived macrophages. Mediators Inflamm 2013: 208412.
44. Cheng-Mayer C, Rutka JT, Rosenblum ML, McHugh T, Stites DP, et al. (1987) Human immunodeficiency virus can productively infect cultured human glial cells. Proc Natl Acad Sci U S A 84: 3526–3530.
45. Ghafouri M, Amini S, Khalili K, Sawaya BE (2006) HIV-1 associated dementia: symptoms and causes. Retrovirology 3: 28.
46. Nomaguchi M, Doi N, Fujiwara S, Saito A, Akari H, et al. (2013) Systemic biological analysis of the mutations in two distinct HIV-1mt genomes occurred during replication in macaque cells. Microbes Infect 15: 319–328.

OPEN ACCESS Freely available online

PLOS | ONE

Slower Uncoating Is Associated with Impaired Replicative Capability of Simian-Tropic HIV-1

Ken Kono[1¤☯], Eri Takeda[1☯], Hiromi Tsutsui[1], Ayumu Kuroishi[1], Amy E. Hulme[2], Thomas J. Hope[2], Emi E. Nakayama[1], Tatsuo Shioda[1*]

1 Department of Viral Infections, Research Institute for Microbial Diseases, Osaka University, Suita, Osaka, Japan, **2** Department of Cell and Molecular Biology, Feinberg School of Medicine, Northwestern University, Chicago, Illinois, United States of America

Abstract

Human immunodeficiency virus type 1 (HIV-1) productively infects only humans and chimpanzees, but not Old World monkeys, such as rhesus and cynomolgus (CM) monkeys. To establish a monkey model of HIV-1/AIDS, several HIV-1 derivatives have been constructed. We previously generated a simian-tropic HIV-1 that replicates efficiently in CM cells. This virus encodes a capsid protein (CA) with SIVmac239-derived loops between α-helices 4 and 5 (L4/5) and between α-helices 6 and 7 (L6/7), along with the entire *vif* from SIVmac239 (NL-4/5S6/7SvifS). These SIVmac239-derived sequences were expected to protect the virus from HIV-1 restriction factors in monkey cells. However, the replicative capability of NL-4/5S6/7SvifS in human cells was severely impaired. By long-term cultivation of human CEM-SS cells infected with NL-4/5S6/7SvifS, we succeeded in partially rescuing the impaired replicative capability of the virus in human cells. This adapted virus encoded a G-to-E substitution at the 116th position of the CA (NL-4/5SG116E6/7SvifS). In the work described here, we explored the mechanism by which the replicative capability of NL-4/5S6/7SvifS was impaired in human cells. Quantitative analysis (by real-time PCR) of viral DNA synthesis from infected cells revealed that NL-4/5S6/7SvifS had a major defect in nuclear entry. Mutations in CA are known to affect viral core stability and result in deleterious effects in HIV-1 infection; therefore, we measured the kinetics of uncoating of these viruses. The uncoating of NL-4/5S6/7SvifS was significantly slower than that of wild type HIV-1 (WT), whereas the uncoating of NL-4/5SG116E6/7SvifS was similar to that of WT. Our results suggested that the lower replicative capability of NL-4/5S6/7SvifS in human cells was, at least in part, due to the slower uncoating of this virus.

Citation: Kono K, Takeda E, Tsutsui H, Kuroishi A, Hulme AE, et al. (2013) Slower Uncoating Is Associated with Impaired Replicative Capability of Simian-Tropic HIV-1. PLoS ONE 8(8): e72531. doi:10.1371/journal.pone.0072531

Editor: Zhiwei Chen, The University of Hong Kong, Hong Kong

Received April 19, 2013; **Accepted** July 10, 2013; **Published** August 13, 2013

Funding: This work was supported by the Japan Society for the Promotion of Science Excellent Young Researcher Overseas Visit Program and grants from the Ministry of Education, Culture, Sports, Science, and Technology; the Ministry of Health, Labour and Welfare, Japan; and the Health Science Foundation. This work also was supported by NIH grants RO1 AI47770 and P50 GM082545 to TJH and F32AI089359 to AEH. The funders had no role in study design, data collection and analysis, decision to publish, or preparation of the manuscript.

Competing interests: The authors have declared that no competing interests exist.

* E-mail: shioda@biken.osaka-u.ac.jp

☯ These authors contributed equally to this work.

¤ Current address: Division of Medical Devices, National Institute of Health Sciences, Tokyo, Japan

Introduction

HIV-1 infection begins with the interaction and fusion of viral and cellular membranes. After fusion, a conical core, consisting of the two viral genomic RNAs and several viral proteins, is released into the cytoplasm of the target cell. The major component of the core is the viral capsid protein (CA). In the cytoplasm, CA eventually dissociates from the viral complex in a process termed uncoating. During this time, reverse transcription (RT) of the viral genomes occurs. The resultant double-stranded DNA associates with viral and cellular proteins, constituting the pre-integration complex (PIC). The PIC migrates into the nucleus, where the viral DNA integrates into the chromosomal DNA of the target cell.

HIV-1 uncoating was thought to occur immediately following viral fusion, as CA was undetectable in RT complexes isolated from infected cells [1–3]. Thus, CA was thought to have only a minor role in HIV-1 infection. However, subsequent reports indicated that mutations in CA decreased HIV-1 infectivity. Most of these CA mutant viruses displayed decreased levels of RT products [4–10]. On the other hand, the mutant virus Q63/67A, which encodes two Gln-to-Ala substitutions in CA, exhibited a defect in nuclear entry [4,11,12]. Changes in core stability caused by some of these CA mutations seem to affect uncoating kinetics, which may result in impaired RT or nuclear